Spatial and temporal variations in surface snow chemistry along a traverse from coastal East Antarctica to the ice sheet summit (Dome A)

Guitao Shi[1,2], Hongmei Ma[2], Zhengyi Hu[2], Zhenlou Chen[1], Chunlei An[2], Su Jiang[2], Yuansheng Li[2], Tianming Ma[2], Jinhai Yu[2], Danhe Wang[1], Siyu Lu[2], Bo Sun[2], and Meredith G. Hastings[3]

[1] Key Laboratory of Geographic Information Science (Ministry of Education), School of Geographic Sciences and State Key Lab of Estuarine and Coastal Research, East China Normal University, Shanghai 200241, China

[2] Polar Research Institute of China, Shanghai 200062, China,

[3] Department of Earth, Environmental and Planetary Sciences and Institute at Brown for Environment and Society, Brown University, Providence, Rhode Island 02912, USA.

*Correspondence to: G Shi (gtshi@geo.ecnu.edu.cn)

Abstract

There is a large variability in environmental conditions across the Antarctic ice sheet, and it is of significance to investigate the snow chemistry at as many locations as possible and over time, given that the ice sheet itself, and precipitation and deposition patterns and trends are changing. The China inland Antarctic traverse from coastal Zhongshan Station to the ice sheet summit (Dome A) covers a variety of environments, allowing for a vast collection of snow chemistry conditions across East Antarctica. Surface snow (the upper ~3 cm, mainly representing the summertime snow) and snow pit samples were collected on this traverse during five campaigns, to comprehensively investigate the spatial and temporal variations in chemical ions (Cl^-, NO_3^-, SO_4^{2-}, Na^+, NH_4^+, K^+, Mg^{2+}, and Ca^{2+}) and the related controlling factors. Results show that spatial patterns of ions in surface snow are consistent among the five campaigns, with Cl^-, Na^+, K^+, and Mg^{2+} decreasing rapidly with distance from the coast and NO_3^- showing an opposite pattern. No clear spatial trends in SO_4^{2-}, NH_4^+, and Ca^{2+} were found. In the interior areas, an enrichment of Cl^- versus Na^+ with respect to seawater composition is ubiquitous as a result of the deposition of HCl, ~~which~~ and nssCl^- (nss, non-sea-salt fraction) can account for up to ~40 % of the total Cl^- budget, while ~~enriched~~ nssK^+ and nssMg^{2+} are mainly associated with terrestrial particle mass. On average, nssCa^{2+} and nssSO_4^{2-} in surface snow account for ~77 and 95 % of total Ca^{2+} and total SO_4^{2-}, respectively. The high proportions of the non-sea-salt fractions of Ca^{2+} and SO_4^{2-} are ~~significantly enriched relative to Na^+,~~ mainly related to terrestrial dust inputs and marine biogenic emissions, respectively. Snow NH_4^+ is mainly associated with marine biological activities, with slightly higher concentrations in summer than in winter. On the coast, parts of the winter snow are characterized with ~~a depletion of~~negative nssSO_4^{2-} values~~versus Na^+~~, and a significant negative correlation between nssSO_4^{2-} and Na^+ in wintertime snow was found, suggesting that sea salts originated from the sea ice. In the interior areas, marine biogenic ~~the negative nss~~SO_4^{2-} still dominated snow SO_4^{2-} ~~signal~~ in winter, leading to significant positive nssSO_4^{2-} values. ~~snow resulted from inputs of sea salts being completely swamped by the contribution of marine biogenic emissions. Ternary plots of Cl^-, Na^+, and SO_4^{2-} suggest that sea salt modification is generally negligible on the coast, while the degree of modification processes to sea salts is high in the interior areas, especially during the summertime.~~ Ion flux assessment suggests an efficient transport of nssSO_4^{2-} to at least as far inland as the ~2800 m contour line. ~~The interannual variations in ion concentrations in surface snow on the traverse are likely linked to the changes in the Southern Indian Ocean low (SIOL) from year to year, and the deepening of the SIOL in summer tends to promote the transport of marine aerosols to Princess Elizabeth Land.~~

1 Introduction

Snow can scavenge the atmospheric chemicals, including sea salts, acids and other organic species, and thereby ice cores can provide the most direct records of the composition of the atmosphere. In Antarctica, the EPICA Dome C ice core encompassed more than 800 ka of sequential glaciochemical data, the longest available records obtained thus far from ice cores (EPICA Community Members, 2004; Wolff et al., 2006; Jouzel et al., 2007; Kaufmann et al., 2010). Major chemical ions are among the core classical measurements in snow and ice due to that they are indicative of a wealth of climate information (e.g., marine biological activity, sea ice extent, and atmospheric circulation pattern). In comparison with trace gases trapped in ice core bubbles, the accurate interpretation of glaciochemical records is challenging since chemicals in the ice can be indicative of a combination of sources, transport strength, and preservation processes. At times, records of a particular species in ice cores can be interpreted differently amongst sites, e.g., sodium (Na^+) variability in ice cores might indicate the changes in sea ice extent or atmospheric meridional transport strength at varied locations (Goodwin et al., 2004; Severi et al., 2017). Therefore, there has been great interest in the determination of sources, mechanisms, and pathways of transport as well as preservation mechanisms of chemicals in snow and ice (e.g., Mahalinganathan et al., 2011; Dixon et al., 2013; Shi et al., 2018a), and a better understanding of snow chemistry is crucial towards an accurate interpretation of glaciochemical records from ice cores.

Snow chemistry has been broadly investigated along traverses during the International Trans-Antarctic Scientific Expedition (ITASE), e.g., DDU to Dome C, coast-interior traverse in Terre Adelie, Syowa to Dome F, Terra Nova Bay to Dome C, 1990 ITASE, and US ITASE in West Antarctica (Legrand and Delmas, 1985; Qin et al., 1992; Mulvaney and Wolff, 1994; Proposito et al., 2002; Suzuki et al., 2002; Dixon et al., 2013), and Bertler et al. (2005) has comprehensively summarized the glaciochemical data across the ice sheet, most of which are for surface snow. Among the major ions, sea salt related ions (e.g., Na^+ and Cl^-), in general, are the most abundant species, and typically exhibit a clear spatial trend, with concentrations falling off sharply with distance from the coast. Sea salts in snow are traditionally thought to be from sea spray in open water, and higher wind speeds (more efficient production and transport) are proposed to be responsible for the higher sea salt concentrations in winter (Delmas, 1992). Recently, sea salt aerosols produced from blowing snow above sea ice is thought to be a major source of sea salt related ions (Wolff et al., 2003; Frey et al., 2020), and this tends to well explain their higher concentrations in the winter snow. Also, it is proposed that sea salt aerosols originated from sea ice can be efficiently transported to central Antarctica (Udisti et al., 2012; Legrand et al., 2017b), and thus sea salts can be a proxy in ice cores for sea ice coverage (Abram et al., 2013 and references therein). Acidic ions such as nitrate and sulfate (NO_3^- and SO_4^{2-}) are typically also abundant ionic species in snow, both of which can be deposited as salts in aerosols, and as gaseous acids. SO_4^{2-} in the snow is mainly from marine biogenic sulfur species, dimethylsulphide (DMS) (Legrand, 1995; 1997), with a small proportion from sea salt aerosols, while large volcanic eruption emissions can episodically contribute to spikes in SO_4^{2-} concentration (Legrand and Delmas, 1987; Jiang et al., 2012; Cole-Dai et al., 2013). Thus, SO_4^{2-} in ice cores can be indicative of ocean productivity in the past (e.g., Wolff et al., 2006). Sources of NO_3^- are sometimes complicated to identify, due to the post-depositional processing after deposition into the snowpack (e.g., photolysis and volatilization), and stratospheric input and tropospheric transport from mid-low latitudes have been proposed to be important sources (Wagenbach et al., 1998b; Savarino et al., 2007; Lee et al., 2014; Shi et al., 2015; Shi et al., 2018a). As for calcium (Ca^{2+}) in snow, both long range transport of terrestrial

particle mass and sea salt aerosols are important sources, and Ca^{2+} in ice cores recovered from interior areas is more likely associated with terrestrial inputs (e.g., Wolff et al., 2006). Terrestrial sources can also contribute to potassium (K^+) and magnesium (Mg^{2+}) in snow, but the contribution proportion varies significantly among sites (Legrand et al., 1988; Khodzher et al., 2014). In comparison with the other species, ammonium (NH_4^+) in ~~the~~ snow has been rarely investigated due to the low concentration, and biogenic emissions in the Southern Ocean and/or mid-latitude biomass burning were proposed to be the major sources, depending on the investigation sites (Legrand et al., 1999; Pasteris et al., 2014). In summary, source identification of ions in Antarctic snow and ice has been conducted intensely, however, the site- and area-specific investigations are needed.

With varied sources and lifetimes, ions in snow often exhibit different seasonal variations, e.g., sea salt related ions show high concentrations in winter, while elevated concentrations of SO_4^{2-} and NO_3^- are frequently observed in summer (e.g., Wagenbach, 1996; Gragnani et al., 1998; Traversi et al., 2004; Shi et al., 2015). Indeed, these ions are frequently taken as seasonal markers for snow pit and ice core dating. On annual to decadal time scales, ion concentrations in snow and ice tend to be associated with changes in transport from year to year (Severi et al., 2009; Weller et al., 2011), and thus large scale atmospheric and oceanic circulation in the Southern Hemisphere, such as the Southern Annular Mode (SAM), Southern Oscillation (SO) and Southern Indian Ocean Dipole (SIOD), could potentially influence variations in ions in ice (Russell and McGregor, 2010; Weller et al., 2011; Mayewski et al., 2017). For instance, the variability of Na^+ in the Law Dome ice core was mostly like associated with interannual changes in SAM that dominates the meridional aerosol transport from mid-latitude sources (Goodwin et al., 2004). In addition, sea ice coverage around Antarctica plays an important role in variations in ions, and larger sea ice coverage is linked with higher sea salt concentrations, as well as non-sea salt SO_4^{2-} ($nssSO_4^{2-}$) concentrations in ice, particularly over glacial-interglacial time scales (Kaufmann et al., 2010; Wolff et al., 2010; Abram et al., 2013). In addition to sources, lifetime, and transport processes, the preservation of ions is an important factor influencing concentrations in snow and ice, particularly the volatile species (e.g., NO_3^- and Cl^-). Post-depositional processes can result in significant losses of volatile species in snow, particularly at sites with low snow accumulation rate (e.g., East Antarctic plateau) (Wagnon et al., 1999; Sato et al., 2008; Shi et al., 2015). In summary, spatial and temporal variations in snow chemistry are influenced by a variety of factors, and further observations of ions in snow are needed to determine the controlling factors for particular times and places.

Although investigations of snow chemistry have been carried out along several overland traverses, many Antarctic areas remain undocumented. In addition, the Antarctic ice sheet itself, and precipitation and deposition patterns and trends are changing, and the investigation of snow chemistry under different environmental conditions and over time is needed. The China inland Antarctic traverse from coastal Zhongshan Station to the ice sheet summit (Dome A) covers a distance of 1256 km in the Indian Ocean sector. The first China inland Antarctic expedition took place in 1999, reaching the site ~300 km from the coast, and in 2005, this traverse extended to Dome A plateau (with elevation ~4100 m), where the oldest ice (~one million-year old) was thought to be preserved (Zhao et al., 2018). This traverse covers a range of environments, e.g., high snow accumulation rate is present on the coast and in some interior areas, and very low accumulation rate is observed on the Dome A plateau. It is noted that some of the interior areas are greatly influenced by persistent wind scour, leading to near zero snow accumulation (Das et al., 2013; Ding et al., 2015). This traverse, thus, provides further opportunity to investigate snow chemistry and its main controlling factors in different environments. In

addition, the Dome A deep ice core reached a depth of 803 m in 2019, and an investigation of snow chemistry in the Indian Ocean sector, especially on the Dome A plateau would be of significance to the interpretation of the deep ice core. Several investigations have been carried out in the past to determine the concentrations and spatial patterns of a few ionic species and trace elements on the traverse (e.g., Li et al., 2016; Du et al., 2019), but limited snow chemistry data were previously available. Additionally, the interannual variations in snow chemistry and the related controlling factors on the traverse are far from understood. Therefore, we used surface snow and snow pit samples collected during five China inland Antarctic scientific expedition campaigns, to determine the spatial and temporal variations in a comprehensive set of ions (Na^+, NH_4^+, K^+, Mg^{2+}, Ca^{2+}, Cl^-, NO_3^-, and SO_4^{2-}) and their controlling factors. This work also presents data on snow chemistry from a less documented area, particularly the Dome A area, providing baseline values of snow ions and records of significance for evaluating potential changes in atmospheric chemistry over Antarctica under a warming climate.

2 Methods

2.1 Sample collection

Snow samples were collected along the traverse from the coast to the ice sheet summit during five Chinese National Antarctic Research Expedition (CHINARE) campaigns (Fig. 1). In January 1999, 107 surface snow samples were collected on the traverse (from coast to the site ~1100 km from the coast; the Chinese inland traverse coverage did not extend to Dome A then). In January and February in the years 2011, 2013, 2015, and 2016, 120, 125, 117, and 125 surface snow samples were collected on the traverse, respectively. In total, 594 snow samples were collected during the five seasons.

Surface snow samples were collected at ~10 km intervals, and the sampling sites are generally >500 m away from the traverse route to avoid possible contamination from expedition team activities. During snow sampling, all personnel wore polyethylene (PE) gloves and face masks, and pushed the high-density polyethylene (HDPE) bottles horizontally into the surface snow layer (~3 cm) in the windward direction. It is noted that the surface snow represents different lengths of time at different locations, considering the wide range of snow accumulation rates on the traverse (Fig. 2(a)). At locations with high snow accumulation rate on the coast, the upper 3 cm of snow may represent deposition from a few weeks, while the surface 3 cm of snow could represent deposition over a few months on Dome A plateau. Also, it is possible that the upper 3 cm of snow can be representative of a single snowfall. Still, the information contained in the surface snow generally indicates summertime conditions, as the sampling took place during late January and February in each season. This allows for an investigation of summer snow chemistry patterns on the traverse.

In addition to surface snow, snow pits were sampled in three representative areas on the traverse (P1, P2, and P3; Fig. 1). P1, located on the coast (76.49 ^{o}E, 69.79 ^{o}S; 46 km from the coast), was sampled in December 2015; P2, located in the interior area (77.03 ^{o}E, 76.42 ^{o}S; 800 km from the coast), was sampled in January 2016; P3, located on Dome A plateau (77.11 ^{o}E, 80.42 ^{o}S; 1256 km from the coast), was sampled in January 2010. Sites P1 and P2 are characterized with high snow accumulation rate (>100 kg m^{-2} a^{-1}), while snow accumulation rate at P3 is ~25 kg m^{-2} a^{-1}. The depths of P1, P2, and P3 are 180, 100, and 150 cm, respectively, with the respective sampling resolution of 5, 3, and 1 cm. Snow pit samples were collected using the narrow mouth HDPE bottles pushed horizontally into the snow wall from the bottom of the pit and moving upwards.

All of the bottles used for snow sampling were pre-cleaned with Milli-Q water (18.2 MΩ), dried in a class 100 super clean hood and then sealed in clean PE bags that were not opened until the field

sampling started. During each sampling campaign, three pre-cleaned bottles filled with Milli-Q water taken to the field and treated to the same conditions as field samples represent field blanks. After collection, the bottles were again sealed in clean PE bags and preserved in clean expanded polypropylene boxes. All samples were transported and stored under freezing conditions (~-20 ^{o}C).

2.2 Sample analysis

Snow samples were first melted in the closed bottles on a super clean bench (class 100) before chemical measurements. In the class 100 room, about 5 ml of the melted sample was transferred to the pre-cleaned 8-ml ion chromatography (IC) autosampler vials, and then the lid was tightly screwed on to the vials. The samples were analyzed by IC for the concentrations of ions (Na^+, NH_4^+, K^+, Mg^{2+}, Ca^{2+}, Cl^-, NO_3^-, and SO_4^{2-}). (Note that the IC was installed in a class 1000 clean room) The samples collected in 1999 were analyzed by using the DX-500 IC system (Dionex, USA), while the snow collected in the other campaigns were analyzed using an ICS-3000 IC system (Dionex, USA). The eluents for cations and anions were methanesulfonic acid (MSA) and potassium hydroxide (KOH), respectively. More details on this method are described in Shi et al. (2012). During sample analysis, replicate determinations (n = 5) were performed, and one relative standard deviation (1σ) for all eight ions was generally <5 %. In addition, the pooled standard deviation ($1\sigma_p$) of all replicate samples run in at least two different sets was examined (n = 65) and yielded 0.020, 0.023, 0.038, 0.022, 0.039, 0.005, 0.008, and 0.005 μeq L^{-1} for Cl^-, NO_3^-, SO_4^{2-}, Na^+, NH_4^+, K^+, Mg^{2+}, and Ca^{2+}, respectively. Ion concentrations in field blanks are lower than the detection limit (DL, 3 standard deviations of water blank in the laboratory).

In Antarctic snow, previous observations suggested that concentrations of H^+ can be reasonably deduced from the ion-balance disequilibrium, if the direct measurements of H^+ are unavailable (Legrand and Delmas, 1984; Legrand and Delmas, 1985; Legrand, 1987). ~~are usually not measured directly, but deduced from the ion-balance disequilibrium in the snow.~~ Here, H^+ concentration is calculated as follows.

$[H^+] = [SO_4^{2-}] + [NO_3^-] + [Cl^-] - [Na^+] - [NH_4^+] - [K^+] - [Mg^{2+}] - [Ca^{2+}]$ Eq. (1),

where ion concentrations are in μeq L^{-1}. In addition, the non-sea-salt fractions of ions (nssX), including $nssCl^-$, $nssSO_4^{2-}$, $nssK^+$, $nssMg^{2+}$, and $nssCa^{2+}$, can be calculated from the following expression,

$[nssX] = [X]_{snow} - ([X]/[Na^+])_{seawater} \times [Na^+]_{snow}$ Eq. (2),

where [X] is the concentration of ion X, and $[X]/[Na^+]$ ratios in seawater are 1.17 (Cl^-), 0.12 (SO_4^{2-}), 0.022 (K^+), 0.23 (Mg^{2+}) and 0.044 (Ca^{2+}) (in μeq L^{-1}). The values of nssX are identical to the concentrations in excess with respect to the seawater composition in previous observations (e.g., Legrand and Delmas, 1985).

~~**2.3 Enrichment assessment of ions**~~

~~The enrichment factor (EF) is a measurement of whether or not an ion is present in a relative abundance similar to that of seawater, which can be calculated as follows.~~

~~$EF_x = ([X]/[Na^+])_{snow} / ([X]/[Na^+])_{seawater}$ Eq. (3).~~

~~When EF > 1.0, the ion X is enriched, i.e., additional sources are present in addition to sea salt spray. EF <1.0 corresponds to the depletion of ion X, possibly indicating the presence of fractionation.~~

~~In both equations (2) and (3), we assume that Na^+ is exclusively from the sea spray (i.e., the sea salt indicator) in surface snow based on the following facts: 1) the Cl^-/Na^+ ratios in snow samples are generally above 1.17, the average value in seawater, 2) the contribution of dust leachable Na is negligible in Antarctic snow, and 3) negligible Na^+ fractionation resulted from mirabilite~~

~~($Na_2SO_4 \cdot 10H_2O$) precipitation in sea ice formation at < -8°C, especially considering the smallest sea ice extent in late summer in East Antarctica.~~

2.~~4~~ 3 Principal component analysis (PCA) of ions

The essence of PCA is converting the observed variables into factors or principal components, so that a minimized set of underlying variables can be identified. Bartlett sphericity test and Kaiser-Meyer-Olkin test indicated that the raw data (i.e., ion concentrations in surface snow) were suitable for PCA ($p<0.001$). Varimax with Kaiser normalization rotation was applied to maximize the variances of the factor loadings across variances for each factor. The regression method was selected for calculating the factor score coefficient. Three components with eigenvalue >1.0 were extracted. The loadings were obtained from the eigenvalues of the three components and their corresponding eigenvectors.

Because the samples collected in 1999 did not cover the whole traverse and the ion concentrations were determined using a different IC system, the ion data of 1999 were excluded in the ~~EF and~~ PCA analysis in the following.

3 Results

3.1 Chemical ion variations in snow pits

Clear seasonal cycles of Na^+ and $nssSO_4^{2-}$ are present in P1 and P2, and thus the two pits can be well dated, spanning ~3 years (Figs. 3 (a) and (b)). Based on the snow pit dating, it is estimated that snow accumulation rate is ~50 (P1) and ~33 cm snow per year (P2), agreeing well with the field measurements (P1: ~150 kg m^{-2} a^{-1}; P2: ~100 kg m^{-2} a^{-1}; Fig. 2(a)), assuming a snow density of ~0.33 g cm^{-3}. At P1, negative $nssSO_4^{2-}$ values are observed in winter snow, i.e., SO_4^{2-}/Na^+ ratio below that of bulk seawater, while all of the $nssSO_4^{2-}$ data in P2 pit are positive. It is difficult to assign the samples in the snow pits to the four distinct seasons based on the measured parameters, and thus, in the following discussion, we choose a conservative assignment method, i.e., a summer season featured with higher $nssSO_4^{2-}$ and SO_4^{2-}/Na^+ ratio (and lower Na^+) and a winter season characterized with the opposite patterns. In addition to SO_4^{2-} and Na^+, the other species also show seasonal variations, especially in pit P1, where elevated levels of NO_3^- and NH_4^+ are generally present in summer snow, and the values of Cl^-, K^+, Mg^{2+}, and Ca^{2+} are high in winter. It is noted that even in the same season, ion concentrations could vary among samples at a single site (e.g., shaded areas in Figs. 3(a) and (b)).

As for $nssSO_4^{2-}$ at P3, the very large signal at the depth of ~120 cm is most likely the fallout from the massive eruption of Pinatubo in 1991 (Fig. 3(c)), based upon previous observations at Dome A (e.g., Hou et al., 2007). Accordingly, the snow accumulation rate from 1992 to 2010 is ~22 kg m^{-2} a^{-1}, in line with previous investigations (Hou et al., 2007; Jiang et al., 2012; Ding et al., 2016). Based on $nssSO_4^{2-}$ signals and the method proposed by Cole-Dai et al. (1997), 19 continuous samples have been identified as influenced by Pinatubo eruption, covering ~2.5 years, possibly suggesting that the effects of Pinatubo eruption on atmospheric chemistry lasted at least for 2.5 years over Dome A. Interestingly, only elevated SO_4^{2-} concentrations are present during this period, and anomalous high or low concentrations of other ions are absent. Additionally, no correlation was found between $nssSO_4^{2-}$ and other species during the 2.5 years, possibly suggesting that Pinatubo volcanic emissions contribute less to the ion budgets other than SO_4^{2-} at Dome A.

Previous investigations proposed that Na^+ and $nssSO_4^{2-}$ in surface snow (top ~1 cm) collected during a full year at central Antarctica show clear seasonal cycles, with high (low) Na^+ in winter (summer)

snow (Udisti et al., 2012). At P3, Na^+, $nssSO_4^{2-}$ and the ratios of SO_4^{2-}/Na^+ fluctuate significantly (Fig. 3(c)), and these contrasts are unlikely indicative of the seasonal cycles as that for P1 and P2. In a full year of snow accumulation at P3, on average, about 7-8 samples were collected, allowing for examining the seasonal variability of ions. Following the field measurements of snow accumulation rate at Dome A during 2008-2011 (~20 kg m^{-2} a^{-1}; Ding et al., 2015), the snow samples covering the years 2008 and 2009 can be roughly identified, assuming an even distribution of snow accumulation throughout the year. In total, there are 7 and 8 samples identified in the years 2008 and 2009, respectively (Fig. S1), and no seasonal cycles in Na^+, $nssSO_4^{2-}$, and SO_4^{2-}/Na^+ ratio were found due to the low snow accumulation rate at P3. In addition, the post-depositional processes (e.g., migration, diffusion, and ventilation processes) and/or wind scouring can obscure the original signal (Cunningham and Waddington, 1993; Albert and Shultz, 2002; Libois et al., 2014; Caiazzo et al., 2016), resulting in the absence of seasonal cycles of ions at P3.

In terms of the non-sea-salt fractions in the snow pits (Fig. S2), $nssCl^-$ is lower at P1 (0.25 ±0.28 μeq L^{-1}) than at the inland sites P2 and P3 (0.42 ±0.18 and 0.58 ±0.34 μeq L^{-1}, respectively), while the concentrations of $nssK^+$, $nssMg^{2+}$, and $nssCa^{2+}$ generally show similar spatial patterns, possibly due to the low snow accumulation rate in interior areas. Different from the sea salt ions and $nssSO_4^{2-}$, $nssCl^-$, $nssK^+$, $nssMg^{2+}$, and $nssCa^{2+}$ in pits P1 and P2, do not show significant seasonal patterns. In the coastal pit P1, the non-sea-salt fractions account for less (<~30%) of the total ions, and the contribution percentages of non-sea-salt fractions increased at inland sites P2 and P3, about 30-70 %.

3.~~1~~ 2 Ion concentrations in surface snow

Concentrations of ions in surface snow collected during the five seasons are shown in Fig. 2, and the ranges (mean) of Cl^-, NO_3^-, SO_4^{2-}, Na^+, NH_4^+, K^+, Mg^{2+}~~–~~, and Ca^{2+} are 0.15-14.6 (1.29), 0.48-12.6 (3.37), 0.37-5.63 (1.52), 0.09-12.74 (0.68), 0.04-0.77 (0.16), 0.01-0.27 (0.04), 0.11-2.76 (0.22), and 0.01-0.50 (0.13) μeq L^{-1}, respectively. These values fall within the reported ranges of the ITASE program sampling (Bertler et al., 2005). Ion concentrations are both spatially and temporally variable, with the coefficient of variation (ratio of one standard deviation over mean) of >0.48, suggesting a large variability across the traverse. In general, ion concentrations do not follow a normal distribution (p>0.05, One-Sample Kolmogorov-Smirnov Test), with the values of skewness and kurtosis above 1.0, but they correspond to a logarithmic normal distribution.

pH values of surface snow sampled in 2013 were measured with a glass pH electrode in a class 100 room at room temperature (~20°C), and H^+ concentrations deduced from pH are correlated well with the values calculated from the ion-balance method (Fig. ~~3~~4(a)). On average, H^+ concentrations obtained from the ion balance approach are ~25 % lower than those deduced from pH. It is noted that pH measurements in this study remain uncertain considering that snow samples are highly undersaturated with respect to carbon dioxide (CO_2) immediately after melting in the lab (Pasteris et al., 2012). On the other hand, organic acids, e.g., monocarboxylic and methanesulfonic acids (MSA), were excluded in H^+ calculation (Eq. 1), although their concentrations in Antarctic snow tend to be very low (Li et al., 2015; Li et al., 2016). If the contribution of organic acids to H^+ in ~~the~~ snow is negligible, the x-intercept of ~2.4 μeq L^{-1} in the linear regression (Fig. 3(a)) can be regarded as the contribution from dissolved CO_2 in snow during pH measurements. This value is close to that of pure water in equilibrium with CO_2 in the atmosphere, with pH=5.6 corresponding to H^+ concentration of ~2.5 μeq L^{-1}. Here, the calculated H^+ concentrations vary in the range of 0.51-10.01 μeq L^{-1}, with a mean of 3.53 ±1.61 μeq L^{-1}. In general, the calculated H^+ values of the coastal surface snow are generally

comparable to previous direct measurements in Terre Adelie (Legrand and Delmas, 1985).

~~The percentage of each constituent to the total ions in surface snow is shown in Fig. 3(b). The most abundant species is H^+, accounting for 39.6 % of the total ions, followed by NO_3^- and SO_4^{2-}, representing 27.5 and 12.5 % of the total ion budget, respectively. The high contribution percentage of H^+ is consistent with previous investigations (Udisti et al., 2004; Traversi et al., 2009; Pasteris et al., 2014), suggesting the acidic characteristics of surface snow. In general, ions NH_4^+, K^+, Mg^{2+}, and Ca^{2+} are the smallest component of the ionic composition, with the four cation summing to ~5 % of the total.~~

~~Previous investigations of ions in surface snow covered various depths among different traverses or campaigns, e.g., 1.0 m deep layer for the traverse from Terra Nova Bay to Dome C and top 25 cm snow for the 1990 ITASE (Qin et al., 1992; Proposito et al., 2002). It is noted that different sampling depths can result in varied ion concentrations in snow. For instance, in inland Antarctica, NO_3^- is often concentrated on the top few centimeter snow, and decreases significantly with increasing depth (Shi et al., 2015). Thus, any comparison of ion concentrations in surface snowpack collected from different campaigns should be made with caution.~~

3.~~2~~ 3 Spatial patterns of ions in surface snow

The spatial distribution patterns of ions on the traverse are consistent among the five campaigns (Fig. 2). In general, Cl^-, Na^+, K^+, and Mg^{2+} show very high concentrations within the narrow coastal region, and decrease sharply further inland, with low values on Dome A plateau (~1000-1250 km from the coast). It is noted that some samples on the coast also show elevated Ca^{2+} concentrations. The spatial patterns are consistent with previous observations (Bertler et al., 2005; Kärkäs et al., 2005), and the high ion concentrations near the coast have been explained by the strong marine air mass intrusions (Hara et al., 2014).

Different from other species, NO_3^- concentrations near the coast are low, and increase towards inland, with the highest values on the Dome A plateau. A significant correlation is found between NO_3^- and distance from the coast, with $r = 0.56$ and $p < 0.001$. The spatial trend of NO_3^- is generally opposite to that of snow accumulation rate on the traverse (Figs. 2(a) and (c)), possibly associated with post-depositional cycling of NO_3^- in surface snow (Erbland et al., 2013; Shi et al., 2018b). Similarly, there is a close relationship between H^+ and distance from the coast ($r = 0.48$, $p < 0.001$), suggesting a higher acidity of inland snow. As for SO_4^{2-}~~,~~ (and $nssSO_4^{2-}$), NH_4^+, and Ca^{2+}, no clear spatial trend was found on the traverse.

It is noted that the surface snow mainly represents the summertime deposition (section 2.1), and therefore the spatial patterns of ions here can only indicate summertime conditions. In addition, the spatial variations of ions in surface snow may arise from the temporal changes in chemical ions, considering that the upper ~3cm corresponds to deposition over different time at varied locations.

Previous investigations of ions in surface snow covered various depths among different traverses or campaigns, e.g., 1.0 m deep layer for the traverse from Terra Nova Bay to Dome C and top 25 cm snow for the 1990 ITASE (Qin et al., 1992; Proposito et al., 2002). It is noted that different sampling depths can result in varied ion concentrations in snow. For instance, in inland Antarctica, NO_3^- is often concentrated on the top few-centimeter snow, and decreases significantly with increasing depth (Shi et al., 2015). Thus, any comparison of ion concentrations in surface snowpack collected from different campaigns should be made with caution.

The percentages of each constituent to the total ions in surface snow on the traverse are shown in Figs. 4(b)-(d). The most abundant species is H^+, accounting for about 30-40 % of the total ions,

followed by NO_3^-, SO_4^{2-}, and Cl^-. In general, ions NH_4^+, K^+, Mg^{2+}, and Ca^{2+} are the smallest component of the ionic composition, with the four cation summing to ~5 % of the total. Spatially, the contribution percentages of H^+ and NO_3^- increase with increasing distance from the coast, with the highest values on Dome plateau (42.3 and 34.5 %, respectively), while Cl^-, Na^+, Mg^{2+}, and NH_4^+ show an opposite pattern and no clear trend was observed for SO_4^{2-}. The high contribution percentage of H^+ is consistent with previous investigations (Udisti et al., 2004; Traversi et al., 2009; Pasteris et al., 2014), and suggests acidic characteristics of summertime surface snow.

~~**3.3 Ions in snow pits**~~

~~Clear seasonal cycles of Na^+ and $nssSO_4^{2-}$ are present in P1 and P2, and thus the two pits can be well dated, spanning ~3 years (Figs. 4(a) and (b)). Based on the snow pit dating, it is estimated that snow accumulation rate is ~50 (P1) and ~33 cm snow per year (P2), agreeing well with the field measurements (P1: ~150 kg m^{-2} a^{-1}; P2: ~100 kg m^{-2} a^{-1}; Fig. 2(a)), assuming a snow density of ~0.33 g cm^{-3}. At P1, negative $nssSO_4^{2-}$ values are observed in winter snow, i.e., SO_4^{2-}/Na^+ ratio below that of bulk seawater, while all of the $nssSO_4^{2-}$ data in P2 pit are positive. It is difficult to assign the samples in the snow pits to the four distinct seasons based on the measured parameters, and thus, in the following discussion, we choose a conservative assignment method, i.e., a summer season featured with higher $nssSO_4^{2-}$ and SO_4^{2-}/Na^+ ratio (and lower Na^+) and a winter season characterized with the opposite patterns.~~

~~As for $nssSO_4^{2-}$ at P3, the very large signal at the depth of ~120 cm is most likely the fallout from the massive eruption of Pinatubo in 1991 (Fig. 4(c)), based upon previous observations at Dome A (e.g., Hou et al., 2007). Accordingly, the snow accumulation rate from 1992 to 2010 is ~22 kg m^{-2} a^{-1}, in line with previous investigations (Hou et al., 2007; Jiang et al., 2012; Ding et al., 2016). Based on $nssSO_4^{2-}$ signals and the method proposed by Cole-Dai et al. (1997), 19 continuous samples have been identified as influenced by Pinatubo eruption, covering ~2.5 years, possibly suggesting that the effects of Pinatubo eruption on atmospheric chemistry lasted at least for 2.5 years over Dome A. Interestingly, only elevated SO_4^{2-} concentrations are present during this period, and anomalous high or low concentrations of other ions are absent. Additionally, no correlation was found between $nssSO_4^{2-}$ and other species during the 2.5 years, suggesting that Pinatubo volcanic emissions contribute less to the ion budgets other than SO_4^{2-} at Dome A.~~

~~Previous investigations proposed that Na^+ and $nssSO_4^{2-}$ in surface snow (top ~1 cm) collected during a full year at central Antarctica show clear seasonal cycles, with high (low) Na^+ in winter (summer) snow (Udisti et al., 2012). At P3, Na^+, $nssSO_4^{2-}$ and the ratios of SO_4^{2-}/Na^+ fluctuate significantly, and these contrasts are unlikely indicative of the seasonal cycles as that for P1 and P2. In a full year of snow accumulation at P3, on average, 7-8 samples were collected, allowing for examining the seasonal variability of ions. Following the field measurements of snow accumulation rate at Dome A during 2008-2011 (~20 kg m^{-2} a^{-1};(Ding et al., 2015), the snow samples covering the years 2008 and 2009 can be roughly identified, assuming an even distribution of snow accumulation throughout the year. In total, there are 7 and 8 samples identified in the years 2008 and 2009, respectively (Fig. 5), and no seasonal cycles in Na^+, $nssSO_4^{2-}$, and SO_4^{2-}/Na^+ ratio were found, maybe related to the post-depositional processes (e.g., migration, diffusion, and ventilation processes) and/or wind scouring that could obscure the original signal (Cunningham and Waddington, 1993; Albert and Shultz, 2002; Libois et al., 2014; Caiazzo et al., 2016).~~

~~–~~

4 Discussions

4.1 ~~Enrichment~~ Non-sea-salt fractions of ions in surface snow

~~Statistics of enrichment factors (EFs) of ions in surface snow are shown in Fig. 6, and EFs ranges (means)~~The positive (negative) nssX values indicate the enrichment (depletion) of an ion with respect to the seawater composition. In surface snow, the non-sea-salt fractions of Cl^-, SO_4^{2-}, K^+, Mg^{2+}, and Ca^{2+} are ~~0.5-6.6 (1.8)~~0.51±0.44, 1.44±0.84~~1.5-87.8 (25.7)~~, 0.03±0.02~~0.7-11.4 (4.6)~~, 0.08±0.06~~0.9-6.2 (2.0)~~, and 0.09±0.08~~0.2-63.2 (7.3)~~, respectively. In the following, we will discuss the non-sea-salt fractions of ions in surface snow by plotting the ions versus Na^+.~~Most EFs of Cl^-, K^+, and Mg^{2+} are close to 1.0, suggesting the main source of sea salt spray, while most EFs of SO_4^{2-} and Ca^{2+} are well above 1.0, i.e., greatly enriched, indicating additional sources. Spatially, EFs of Cl^-, K^+, Mg^{2+}, and Ca^{2+} at the sites close to the coast are around 1.0, with elevated values in interior areas, especially on the Dome A plateau.~~

Correlation plots of ions versus Na^+ in surface snow are shown in Fig. ~~7~~5, and the plots above (below) the seawater dilution line represent the enrichment (depletion) of the ions. The further the plots deviate away from the line, the higher degree of enrichment or depletion of the ions. On the coast, most of the Cl^-/Na^+ data are distributed close to the seawater dilution line (Fig. ~~7~~5(a)), indicating a quantitative sea salt tracer of snow Cl^-, while most of the plots in the interior areas are above the seawater line, suggesting an enrichment of snow Cl^-. On this traverse, $nssCl^-$ accounted for an average of 38 % of total Cl^-, with lower (higher) percentages on the coast (plateau), generally in line with previous reports (e.g., Suzuki et al., 2002). The modifications in Cl^- with respect to bulk seawater can occur via the heterogeneous reactions, as follows (Finlayson-Pitts, 2003),

$NaCl + H_2SO_4 = HCl + Na_2SO_4$ (R1)

$NaCl + HNO_3 = HCl + NaNO_3$ (R2)

In the atmosphere, the production of HCl will result in depletion of Cl^- in sea salt aerosol. The 'secondary' HCl, in the gas phase and/or fine aerosol mode, can be transported further inland due to the longer lifetime (versus the coarse sea salt aerosols removed preferentially from the atmosphere). In this case, an enrichment of Cl^- would be expected in the inland snowpack. On the other hand, Cl^- is not irreversibly deposited to the snow, and it can be released back into the atmosphere through the formation of HCl, resulting in an enrichment of Cl^- in surface snow via re-deposition. Post-depositional losses of HCl are thought to be associated with snow accumulation rate, with larger losses occurring at sites with snow accumulation generally <40 kg m^{-2} a^{-1} (Röthlisberger et al., 2003). Indeed, a negative correlation was found between snow accumulation and $nssCl^-$ (Fig. ~~8~~6(a)) for most interior areas that featured low snow accumulation and consequently an enhanced cycling of Cl^-.

Different from Cl^-, Mg^{2+} is irreversibly deposited into the snow. Most of the Mg^{2+}/Na^+ data points are above or close to the seawater dilution line, similar to that of Cl^-/Na^+ (Fig. ~~7~~5(d)). On the coast, Mg^{2+}/Na^+ data points are in general close to the seawater dilution line, suggesting the main source is sea salt aerosols, while most of the inland samples are slightly enriched with Mg^{2+}, agreeing with previous observations (e.g., Dome F; Hara et al., 2014). The fraction of $nssMg^{2+}$, on average, represents ~36 % of Mg^{2+} in snow, with lower (higher) values on the coast (plateau). The enrichment of Mg^{2+} has not been observed in sea salt particles produced by bubble bursting (Keene et al., 2007), and thus enriched Mg^{2+} in the snow is unlikely associated with sea salt spray. In the atmosphere, sea salt aerosols would also be modified at low temperatures via the formation of mirabilite (R1), thus leading to an elevated ratio of Mg^{2+}/Na^+ if mirabilite precipitate from the aerosols. However, the solid-liquid separation of mirabilite in the aerosol droplet was not observed in the experiments (Wagenbach et al.,

1998a). Thus, the enrichment of Mg^{2+} in surface snow is unlikely associated with sea salt fractionation. Although it is proposed that Mg^{2+} separation in sea salts can occur in surface snow due to the re-freezing process on surface snow (i.e., the quasi-liquid layers on the crystal surface can act like seawater freezing; Hara et al., 2014), our measurement of Mg^{2+} in bulk snow is unlikely to support this process responsible for Mg^{2+} enrichment. A previous observation conducted near this traverse showed a moderate correlation of Mg^{2+} with element Al in the surface snowpack (r=0.53, p<0.05), indicating a contribution of continental dust (Khodzher et al., 2014). Thus, the most plausible interpretation of enriched Mg^{2+} in surface snow is the contribution of terrestrial aerosols.

Similar to Mg^{2+}, most of K^+/Na^+ data points are close to the seawater dilution line on the coast, suggesting a primary contribution of sea salt spray (Fig. ~~7~~5(c)). Slightly enriched K^+ was present in inland snow, possibly indicating other sources such as biological activity on the coast, mineral transport, and combustion emissions in Southern Hemisphere (Rankin and Wolff, 2000; Virkkula et al., 2006; Hara et al., 2013). Given that the sampling sites are at least several tens of kilometers away from the coast, the contribution of biological activity to snow K^+ would be rather minor (Rankin and Wolff, 2000). A previous investigation of the atmospheric particles suggests a contribution of combustion in South America and Southern Africa to atmospheric K^+ in Antarctica (Hara et al., 2013). Indeed, aerosol particles from biomass burning in the Southern Hemisphere can be transported to Antarctica, resulting in the ubiquitous distribution of biomass burning tracers observed in the snow on this traverse (Shi et al., 2019). Here, no elevated snow $nssK^+$ peaks were found in austral autumn (i.e., P1 and P2; Fig. S2) when the chemicals emitted from biomass burning (e.g., black carbon) often peaked in Antarctic snow (Sigl et al., 2016). In addition, there is a close relationship between $nssK^+$ and $nssCa^{2+}$ (r=0.22, p<0.001), suggesting that snow $nssK^+$ is unlikely dominated by biomass burning emissions. ~~However, the average ratio of $nssK^+/nssCa^{2+}$ (~0.29) on the traverse is slightly higher than that of the average crust, likely supporting a minor contribution of biomass burning emissions. If $nssK^+$ in surface snow is exclusively from terrestrial minerals and combustion processes, it is estimated that ~10 % of $nssK^+$ is originated from biomass burning emissions.~~

域代码已更改

Positive $nssCa^{2+}$ is generally ~~enriched versus Na^+~~ present on the traverse, with most of the Ca^{2+}/Na^+ data points above the seawater dilution line, especially at inland sites (Fig. ~~7~~5(e)). The fraction of $nssCa^{2+}$, on average, accounts for ~77 % of total Ca^{2+} in surface snow, indicating other dominant sources. In Antarctica, snow $nssCa^{2+}$ has been thought to be mainly associated with terrestrial inputs (Bertler et al., 2005; Wolff et al., 2010). Previous modeling studies suggest that the dust mass reaching East Antarctica mainly originates from South America, specifically Patagonia (Basile et al., 1997; Wolff et al., 2006; Mahalinganathan and Thamban, 2016). Metal isotopes in snow collected on this traverse suggested that Australian mineral dust also can contribute to snow particles (Du et al., 2018). In addition, Antarctic ice free areas were thought to be a contribution to snow dust (Delmonte et al., 2013; Du et al., 2018). If the dust mass originated from ice free area near the coast and dominated $nssCa^{2+}$, then $nssCa^{2+}$ concentrations near the coast would be expected to be higher, while the data shows the opposite. Thus, terrestrial dust mass, possibly from both South America and Australia likely dominates snow $nssCa^{2+}$. It is noted that some Ca^{2+} concentrations in surface snow (e.g., coastal and some inland sites) are above 0.2 μeq L^{-1}(Fig. 2(i)), slightly higher than most reports of snow and ice under present-day climate (e.g., Legrand and Mayewski, 1997). On the coast, the high concentrations could be related to marine inputs (e.g., Bertler et al., 2005), while the elevated values in the inland regions (about 500-900 km from the coast, where the glaze/dune are distributed) are possibly associated with the low and fluctuating snow accumulation rate due to the strong wind scouring (Ding

et al., 2011; Das et al., 2013). Similarly, in the glaze/dune regions on the US ITASE traverses across East and West Antarctica, concentrations of Ca^{2+} in snow and ice are also often above ~0.2μeq L^{-1} (Dixon et al., 2013).

Positive nssSO_4^{2-} is ~~greatly enriched~~present in all surface snow (Fig. ~~7~~5(b)), together with the minimum sea ice coverage around East Antarctica in late summer (Holland et al., 2014), suggesting that sea salts in surface snow are from open seawater rather than from the sea ice. On the traverse, nssSO_4^{2-} represents 33-99 % (mean=95 %) of total SO_4^{2-} in surface snow, with lower (higher) proportions on the coast (plateau). In Antarctica, nssSO_4^{2-} essentially originates from marine biogenic production of DMS (Saltzman, 1995) and occasionally from explosive volcanism (Cole-Dai et al., 2000; Cole-Dai et al., 2013). In this study, the significant enrichment of SO_4^{2-} suggests a dominant role of ocean bioactivities. Different from the coarse sea salt aerosols, nssSO_4^{2-} can form fine aerosol particles in the atmosphere (Legrand et al., 2017a), resulting in long atmospheric residence time (>10 days to weeks) and consequently efficient transport (Bondietti and Papastefanou, 1993; Hara et al., 2014). This can help explain the elevated deposition flux of nssSO_4^{2-} frequently found at inland Antarctic sites, e.g., site P2 (discussed below). On this transect, a negative relationship was found between snow accumulation rate and SO_4^{2-} (or nssSO_4^{2-}) (Figs. ~~8~~6(c) and (d)), suggesting that snow accumulation rate can influence snow SO_4^{2-} concentration, possibly via dilution effects, but overall <~10 % of the variation in SO_4^{2-} concentrations can be explained by the relationship.

The ternary diagram of Cl^-, Na^+, and SO_4^{2-} can well characterize the modification processes to sea salt aerosols, and the ternary plot of the three ions in surface snow is shown in Fig. ~~9~~7. The values of the ions were normalized via the following equation,

$X=[X]/([Na^+]+[Cl^-]+[SO_4^{2-}])$ Eq. (~~4~~3),

where [X] is the concentration of ion X in the snow (in μeq L^{-1}). The dashed line between the seawater reference value and the SO_4^{2-} vertex represents the sea salt aerosol composition with additional SO_4^{2-}, i.e., the ratio of Cl^-/Na^+ keeps constant (1.17) with additional SO_4^{2-} along the dashed line. The presence of acids (HNO_3 and H_2SO_4) would result in the liberation of HCl into the atmosphere via reactions R1 and R2, resulting in the changes in Cl/Na ratios, i.e., either Cl^- loss or gain are located right or left of the line, respectively. It is shown that all of the data points are above the seawater plot, suggesting an enrichment of SO_4^{2-} in surface snow. Most of the data points are located left of the line, indicating the general enrichment of Cl^- due to reactions R1 and R2 occurring in the atmosphere and/or in the snowpack. But the coastal data points are generally close to the line, suggesting that the degree of sea salt modification is generally low in the snow.

4.2 Groups of ions in surface snow

PCA is a powerful tool for identifying the common sources and/or transport process of chemicals in different environments. The PCA results (i.e., loadings in each PC), communalities, initial eigenvalues, and explained cumulative percent of the ions in surface snow are listed in Table 1. The first three PCs accounted for 76 % of the variation of the eight original variables. PC1 accounts for 46 % of the variance and is highly loaded by Cl^-, Na^+, K^+, and Mg^{2+}, with the factor loadings higher than 0.7. In addition, the four species are correlated well with each other (Table 2), suggesting the variation of the four species is dominated by sea salt aerosols~~, consistent with the EFs results. Thus, PC1 is indicative of the origin of sea salt aerosols.~~ PC2 accounts for 17 % of the total variance, and the loading values of NH_4^+ and Ca^{2+} in PC2 are high, ~0.8. Ca^{2+} is mainly from terrestrial particle mass, while NH_4^+ is thought to be mainly associated with biological decomposition of organic matter in the Southern Ocean

(Johnson et al., 2007; Kaufmann et al., 2010). In addition, biomass burning from mid-latitudes can contribute to snow NH_4^+ at some sites (Pasteris et al., 2014), and the penguin colony emissions can be important inputs to NH_4^+ in snow several km from the colony (Rankin and Wolff, 2000). On this traverse, no correlation was found between NH_4^+ and biomass burning tracers (e.g., black carbon and phenolic compounds) in surface snow (Shi et al., 2019; Ma et al., 2020), suggesting a minor role of biomass burning emissions. Thus, the high NH_4^+ concentrations on the coast are likely associated with marine biogenic emissions. In this case, it is possible that a similar transport pathway (i.e., preferentially transported long distance in free transport; Krinner and Genthon, 2003; Kaufmann et al., 2010; Krinner et al., 2010) can explain, at least in part, the positive loadings of both NH_4^+ and Ca^{2+} in PC2.

~~In Antarctic snow, NH_4^+ is thought to be mainly associated with biological decomposition of organic matter in the Southern Ocean (Johnson et al., 2007; Kaufmann et al., 2010). In addition, biomass burning from mid-latitudes can contribute to snow NH_4^+ in West Antarctica (Pasteris et al., 2014). On this transect, no correlation was found between NH_4^+ and biomass burning tracers on the traverse (Shi et al., 2019), suggesting a minor role of biomass burning emissions. Thus, NH_4^+ in surface snow tends to be dominated by marine biological activities, and elevated NH_4^+ concentrations in summer snow would be expected, e.g., summer mean of 0.23 μeq L^{-1} versus winter mean of 0.16 μeq L^{-1} at P1 (Fig. S1). It is proposed that the transport of NH_4^+ via free troposphere is an important pathway (Kaufmann et al., 2010). Similarly, the meridional transport of particle mass from continents to Antarctica is more efficient in the mid-troposphere (Krinner and Genthon, 2003; Krinner et al., 2010; Shi et al., 2019). Thus, the shared transport process may explain, at least in part, the positive loadings of NH_4^+ and Ca^{2+} in PC2.~~

NO_3^- is highly loaded in PC3, which accounts for 13 % of the system variance. On this traverse, NO_3^- in the snow has been extensively investigated, and it is proposed that NO_3^- concentrations were influenced by post-depositional processing which is largely dependent on snow accumulation rate (Shi et al., 2015; Shi et al., 2018a; Shi et al., 2018b). A negative relationship was found between NO_3^- and snow accumulation rate (Fig. ~~8~~6(b)), suggesting a high degree of NO_3^- cycling driven by photolysis at low snow accumulation sites.

SO_4^{2-} did not show high loadings in any of the three extracted components. Its positive loading in PC1 (0.55) and weak relationships between SO_4^{2-} and sea salts (Cl^- and Na^+) likely supports the contribution of sea salt aerosols, although a minor one. A positive loading of SO_4^{2-} is also present in PC3 (0.42), and a weak correlation was found between SO_4^{2-} and NO_3^-. Both SO_4^{2-} (or $nssSO_4^{2-}$) and NO_3^- are negatively correlated with snow accumulation rate (Fig. 6), but with distinct mechanisms. $nssSO_4^{2-}$ can be concentrated due to dry deposition at sites with low snow accumulation rate, while elevated NO_3^- concentrations are linked to the photochemical cycling and re-deposition (discussed above). In addition, $nssSO_4^{2}$ and NO_3^- are mainly associated with the secondary aerosols, and the production of both species in summer is closely related to the oxidants HO_x, RO_x, etc (Ishino et al., 2017; Shi et al., 2018a), which may also contribute to the correlation between SO_4^{2-} and NO_3^-. ~~In summer, snow NO_3^- is mainly produced locally considering that the long-range transported nitrogen compounds can decompose and undergo rapid NO_x cycling in the local boundary layer, and NO_3^- production is closely related to the atmospheric oxidants. Although the main production pathways of NO_3^- and SO_4^{2-} are different from each other, their formations are closely related to certain oxidant abundances in the atmosphere (e.g., OH radical), which may partly account for the positive loading of SO_4^{2-} in PC3.~~

4.3 Ions ~~fluxes and enrichment~~ in snow pits: fluxes and the non-sea-salt fractions

In this section, we discuss the fluxes and the non-sea-salt fractions~~enrichment~~ of ions at different depths (i.e., summer and winter snow) in the three snow pits. The bottom ~30 cm layer of P3 will be excluded in the discussion, since it represents a snow layer clearly impacted by volcanic (Pinatubo) eruption emissions.

Ion fluxes in snow can be determined by multiplying the concentrations by snow accumulation rate, and the results in the 3 snow pits are shown in Fig. ~~10~~8. The highest fluxes of ions except for NO_3^- were present at P1, followed by P2 and P3. The flux of NO_3^- shows a different pattern, with the highest value at P2, possibly due to the redistribution of NO_3^- across the Antarctic ice sheet driven by photolysis (Shi et al., 2018b). It is noted that $nssSO_4^{2-}$ fluxes at P1 (99.4±46.7 μeq m^{-2} a^{-1}) and P2 (109.2±21.6 μeq m^{-2} a^{-1}) are comparable, although P1 is located on the coast and P2 located further inland (~800 km from the coast). In addition, the ratio of $nssSO_4^{2-}$ flux at P1 over that at P3 is 2.2, the lowest value among the ratios for the observed ions (17.2, 7.5, 26.7, 8.5, 17.4, 17.0, and 10.0 for Cl^-, NO_3^-, Na^+, NH_4^+, K^+, Mg^{2+}, and Ca^{2+}, respectively), suggesting more efficient transport of $nssSO_4^{2-}$. In other words, atmospheric $nssSO_4^{2-}$ from the open ocean can be efficiently transported to at least as far inland as ~800 km from the coast (~2800 m above sea level; site P2).

At P1, the plots of Cl^-, K^+, Mg^{2+}, and Ca^{2+} versus Na^+ are all close to the bulk seawater dilution line (Fig. ~~11~~9), with ~~EFs of the four species generally below 3. In addition,~~ the slope values of the linear regression between Na^+ and the four ions ~~are~~ close to those of seawater, suggesting a dominant source of sea salt aerosols. In addition, the non-sea-salt fractions of Cl^-, K^+, Mg^{2+}, and Ca^{2+} are 0.25±0.27, 0.02±0.01, 0.04±0.07, and 0.09±0.06 μeq L^{-1}, respectively, contributing less to the total ion budgets. As for SO_4^{2-} in the snow, the proportion of $nssSO_4^{2-}$ to SO_4^{2-} is much higher in summer (~86 %) than in winter (~27 %). All $nssSO_4^{2-}$ in summer snow is positive, while some winter snow samples featured negative $nssSO_4^{2-}$, i.e., SO_4^{2-}/Na^+ ratio below the value of seawater (Fig. ~~4~~3(a)), suggesting sea salt aerosols in winter from sea ice (Marion et al., 1999). In the winter snow, if all of the SO_4^{2-} is from sea salt aerosols, $nssSO_4^{2-}$ is expected to be lower than or close to zero. However, 13 out of the 17 samples classified as winter snow at P1 were characterized with positive $nssSO_4^{2-}$, suggesting a significant contribution from marine biogenic emissions. It is interesting that $nssSO_4^{2-}$ has a strong negative correlation with Na^+ in winter snow ($r=0.82$, $p<0.001$), raising two potential cases: 1) stronger winds transport more sea salt aerosols to P1 featured with depleted SO_4^{2-} from sea ice, thereby resulting in low concentrations of $nssSO_4^{2-}$ and assuming a stable SO_4^{2-} input flux from marine biogenic emissions; and/or 2) with a larger extent of sea ice and strong transport, a large sea salt flux would still result but carry less $nssSO_4^{2-}$ from marine biogenic emissions due to the longer transport distance (Wolff et al., 2006 and references therein). If case 2) dominated $nssSO_4^{2-}$ variations in the winter snow, lower $nssSO_4^{2-}$ would be expected in the end than at the beginning of winter when a sea ice coverage minimum is present. The observation at P1, however, does not support this expected season trend (Fig. ~~S2~~3a). It is most likely, then, that sea salt aerosol inputs dominate $nssSO_4^{2-}$ variations in the winter snow instead of the marine biogenic emissions. In addition, NH_4^+ concentration at P1 (0.16±0.05 μeq L^{-1}) is slightly higher than the previous reports of ice cores but comparable to some coastal observations (e.g., coastal sites in Terre Adelie) (Legrand and Delmas, 1985; Legrand et al., 1998), possibly associated with marine biogenic emissions (i.e., close to the coast) (discussed above).

The patterns of relationships between ions and Na^+ at P2 are similar to those of P1 except for Ca^{2+} (Fig. ~~11~~9). ~~EFs~~ The non-sea-salt fractions of Cl^-, K^+, and Mg^{2+} at P2 are ~~1.5~~0.42 ~~±0.2~~0.18,

~~1.4~~0.005 ~~±0.5~~0.008, and ~~1.5~~0.06 ~~±0.3~~0.02 μeq L^{-1} ~~(mean±1σ)~~, respectively, accounting for less of the total ion concentrations. ~~suggesting again a main source of sea salt aerosols. EFs of Cl^- are slightly higher in summer snow (1.57) than in winter snow (1.47), possibly indicating the presence of elevated H_2SO_4 and HNO_3 during summer promoting the production of HCl via R1 and R2 (discussed above).~~ $nssCa^{2+}$, 0.13 ±0.01 μeq L^{-1}, accounts for 78 % of total Ca^{2+} in snow pit P2, suggesting a dominant role of the terrestrial source. Different from the other species, Ca^{2+} ~~is enriched in P2 (EFs=6.1±2.8), and it~~ remains relatively constant with increasing Na^+ (Fig. ~~11~~9), possibly suggesting seasonal variations in terrestrial dust inputs are insignificant. As for SO_4^{2-}, it is significantly enriched~~, with the EFs of 18.6±11.4~~, and the fractions of $nssSO_4^{2-}$ to SO_4^{2-} in summer and winter snow are 95 and 89 %, respectively. The very high SO_4^{2-} to Na^+ ratio in winter (~1.6, versus 0.12 of bulk seawater) suggests that marine biogenic emissions dominate SO_4^{2-} other than the sea salt aerosols, different from that at P1. It is suggested that the sea salt aerosol flux from the sea ice in winter is much lower in the inland Antarctica than on the coast. Previous investigations proposed that sea salt aerosols emitted from sea ice are an important contribution to sea salt budget in central Antarctica in winter (Levine et al., 2014; Legrand et al., 2016; Legrand et al., 2017b). Here, our data indicate that marine emissions could also be an important source.

At P3, Cl^-, K^+, and Mg^{2+} are correlated well with Na^+ (Fig. ~~11~~9), and the non-sea-salt fractions ~~EFs~~ of the 3 ions are ~~2.1~~0.58 ~~±1.0~~0.34, ~~2.6~~0.02 ~~±1.3~~0.01, and ~~2.0~~0.12 ~~±0.8~~0.04 μeq L^{-1}, respectively, higher than those of P2. Although the sea salt fractions of Cl^-, K^+, and Mg^{2+} account for most of their total budgets in the snow, the other sources can occasionally be important. On average, $nssCl^-$ accounts for ~40 % of the total Cl^-, suggesting that, Cl^- at Dome A is mainly from the sea salt aerosols, but the deposition of HCl is also an important contribution. This percentage is higher than that at P2 (~30 %), suggesting a more important role of HCl on Cl^- budget in further inland snow. At P3, $nssCa^{2+}$ accounts for 75 % of total Ca^{2+} ~~is enriched noticeably at P3, with EFs of 6.6±5.0~~, close to that of P2, suggesting the terrestrial particle mass as the primary source. In terms of SO_4^{2-}, ~~it is enriched significantly (EFs of 27.4±17.3), and~~ the non-sea salt fraction accounts for ~95 % of total SO_4^{2-}, comparable to that of P2. At P2 and P3, ~~the negative nss~~SO_4^{2-} in both summer and winter snow is dominated by marine biogenic emissions (i.e., no negative $nssSO_4^{2-}$ observed), ~~signal resulted from sea salt aerosols originated from sea ice has been completely swamped by the biogenic SO_4^{2-},~~ generally in line with the observation at Dome C (Udisti et al., 2012).

Similar to the surface snow, the modification processes to sea salt aerosols is negligible in snow pit P1, while the ubiquitous modification process to sea salts throughout the year was found in the interior areas (P2 and P3; Fig. S3). Thus, Cl^- in inland Antarctica, often deviating from the seawater dilution line remarkably in both summer and winter, is not a quantitative indicator of sea salts in snow.

~~The ternary plots of Cl^-, Na^+, and SO_4^{2-} at the three pits are shown in Fig. 12. At P1, all plots are close to the seawater composition line, suggesting the modification processes to sea salt aerosols is negligible, similar to that of coastal surface snow. Several winter snow samples at P1 show a depletion of SO_4^{2-} relative to seawater, associated with the precipitation of mirabilite during sea ice formation, while more additional SO_4^{2-} is present in summer snow (Fig. 12(a)). In general, patterns of the three ions at P2 are similar to those of P1, but with Cl^- enriched, especially in summer snow (Fig. 12(b)). Similarly, enriched Cl^- was observed at P3 (Fig. 12(c)), associated with scavenging of HCl in the atmosphere by snow. Such a pattern implies the ubiquitous modification process to sea salts in inland Antarctica throughout the year (via R1 and R2). Together with the surface snow observations (Fig. 9), Cl^- in the interior areas, often deviating from the seawater dilution line remarkably, is not a quantitative~~

indicator of sea salts in snow. At P3, the data points are closer to the SO_4^{2-} summit in comparison with the other two sites, possibly suggesting predominant H_2SO_4 scaveng

4.4 Interannual variations of ions in surface snow

As the snow sampling protocols (e.g., sampling snow depth and intervals) on the traverse are the same in different years, we can directly compare ion concentrations in surface snow collected during different campaigns. Independent samples t test showed that concentrations of Cl^-, Na^+, K^+, Mg^{2+}, and SO_4^{2-} in surface snow are generally higher in 2015 than in the other years, while Ca^{2+} exhibited an opposite pattern ($p<0.05$; Table S1). (2019 data are from personal communication with S. Lu, 2020) Averaged ion concentrations in surface snow collected in different campaigns are shown in Fig. 13.

As for the sea salt related ions in surface snow, i.e., Cl^-, Na^+, K^+, and Mg^{2+}, their concentrations are largely dependent on the transport strength of sea salt aerosols from the oceans, which is strongly linked to large scale atmospheric and oceanic circulation at the high southern latitudes We hypothesize that snow sea salt concentrations in Princess Elizabeth Land (PEL), where most of the investigation sites in this study are located (Fig. 1), are related to the variations in the sea level pressure over the Southern Indian Ocean, specifically the Southern Indian Ocean low (SIOL), a quasi stationary climatological feature located north of Prydz Bay. To test this hypothesis, interannual variation in the SIOL during the study period was examined with the aid of the ERA interim reanalysis. To quantify the strength of the SIOL, the circulation indices of a closed pressure system, including the area index (S) and strength index (P), were calculated following. Considering that the sampling time was January and February, the austral summertime mean sea level pressure was used to calculate the circulation indices in each year (Fig. S3). It is shown that the SIOL is stronger in the austral summer of 2014/2015, i.e., the larger area and the greater strength of SIOL (Fig. S3(f)). A significant correlation was found between the area index of SIOL (S) and Na^+ ($r=0.89$, $p=0.03$; Fig. 13(a)). Accordingly, the higher concentrations of sea salts observed in 2015 can, at least in part, be explained by the SIOL anomaly. Indeed, the marine air mass intrusion into the continent is associated with large scale boundary layer turbulence over the ocean or blocking anticyclones and higher snow sea salt concentrations in coastal PEL were generally connected to the deepening of SIOL (Xiao et al., 2004).

Similar to the temporal patterns of sea salts, higher SO_4^{2-} (and $nssSO_4^{2-}$) concentrations were also observed in 2015. This is likely associated with the fact that SO_4^{2-} in surface snow is mainly from marine biogenic emissions, and a stronger SIOL would also promote the transport of SO_4^{2-}. Interestingly, Ca^{2+} exhibits the lowest concentration in 2015, which may be related to that Ca^{2+} is mainly originated from the mid latitude terrestrial particle mass, instead of the Southern Ocean emissions. A stronger polar low (e.g., SIOL) usually corresponds to strengthening westerly winds, and thereby would result in weaker meridional transport from the mid latitude

It is noted that the observation covers a relatively short period of time, and changes in snow accumulation rate and transport strength from year to year are also likely to influence the variability of ions on an interannual timescale. Thus, there is still uncertainty on the relationships between ion concentrations and the SIOL. During the observation period (2011-2019), however, the SIOL is likely an important factor influencing the interannual variability of major ions in surface snow on the traverse.

5 Conclusions

Surface snow and snow pit samples collected on a traverse from coastal Zhongshan Station to the ice

sheet summit, East Antarctica, during five campaigns were used to comprehensively investigate spatial and temporal variations in snow chemistry. It is shown that Cl^-, Na^+, K^+, and Mg^{2+} concentrations are high within the narrow coastal region, falling off strongly further inland, while NO_3^- exhibits an opposite trend and no clear spatial trends were found for SO_4^{2-}, NH_4^+, and Ca^{2+}. In inland snow, Cl^-, K^+, and Mg^{2+} are slightly enriched relative to Na^+ with respect to the composition of seawater. ~~The enrichment of~~ nssCl^- is ~~likely~~ associated with the deposition of HCl produced from dechlorination of sea salt aerosols, and ~~enriched~~ nssK^+ and nssMg^{2+} are possibly linked to terrestrial particle mass. Ca^{2+} and SO_4^{2-} are significantly enriched versus Na^+, and terrestrial dust mass and marine biogenic emissions are responsible for the enrichments respectively. Snow NH_4^+ is related to marine biological activities, and multivariate statistical analysis suggests, at least in part, the NH_4^+ transport is via free troposphere.

~~In~~ On the coast~~al snow pit~~, parts of the winter snow showed a depletion of SO_4^{2-} versus Na^+, indicating sea salt aerosols sourced from sea ice. In the interior areas, SO_4^{2-} in both summer and winter snow is dominated by marine biogenic emissions, with no negative nssSO_4^{2-} values observed. ~~although sea salt aerosols originated from sea ice contribute to a significant depletion of SO_4^{2-}, the negative nssSO_4^{2-} signal has been completely swamped by the contribution from biogenic SO_4^{2-}.~~ In ~~addition~~general, the contribution proportions of nssCl^- to total Cl^- are higher in interior snow than in coastal snow.~~in the snow is more enriched in summer than in winter, possibly related to more HCl formation due to elevated acid concentrations during summertime.~~ Ternary plots of Cl^-, Na^+~~-~~, and SO_4^{2-} in snow suggest the modification process to sea salts is negligible on the coast, while the degree of modification to sea salts is higher in inland throughout the year, which results in Cl^- not being a quantitative indicator of sea salts. Ion flux assessment suggests an efficient transport of nssSO_4^{2-} to at least as far inland as the ~2800 m contour line.~~ With the aid of reanalysis, it is found that the interannual variations in ion concentrations in surface snow are likely connected to changes in the Southern Indian Ocean low from year to year.~~

Data availability. This dataset, chemical data on ion concentrations in snow on the traverse from coast (Zhongshan Station) to Dome A, is in the process of being hosted on a public server by the Chinese National Arctic and Antarctic Data Center (https://www.chinare.org.cn/).

Author contributions. GS, ZC, YL and BS designed the experiments and GS, HM, ZH, CA, SJ, TM, JY, DW and SL carried them out. GS and MH prepared the manuscript with contributions from all co-authors.

Competing interests. The authors declare that they have no conflict of interest.

Acknowledgements

This research was supported by the National Science Foundation of China (Grant Nos. 41922046 and 41576190 to GS; Grant No. 41876225 to HM) and the National Key Research and Development Program of China (Grant Nos. 2016YFA0302204 and 2019YFC1509102 to GS). The authors are grateful to the CHINARE inland members for logistic support and assistance.

References

Abram, N.J., Wolff, E.W., Curran, M.A.J., 2013. A review of sea ice proxy information from polar ice cores. Quaternary Sci. Rev. 79, 168-183.

Albert, M.R., Shultz, E.F., 2002. Snow and firn properties and air–snow transport processes at Summit, Greenland. Atmos. Environ. 36, 2789-2797.

Basile, I., Grousset, F.E., Revel, M., Petit, J.R., Biscaye, P.E., Barkov, N.I., 1997. Patagonian origin of glacial dust deposited in East Antarctica (Vostok and Dome C) during glacial stages 2, 4 and 6. Earth Planet. Sci. Lett. 146, 573-589.

Bertler, N., Mayewski, P.A., Aristarain, A., Barrett, P., Becagli, S., Bernardo, R., Bo, S., Xiao, C., Curran, M., Qin, D., 2005. Snow chemistry across Antarctica. Ann. Glaciol. 41, 167-179.

Bondietti, E.A., Papastefanou, C., 1993. Estimates of residence times of sulfate aerosols in ambient air. Sci. Total Environ. 136, 25-31.

Caiazzo, L., Becagli, S., Frosini, D., Giardi, F., Severi, M., Traversi, R., Udisti, R., 2016. Spatial and temporal variability of snow chemical composition and accumulation rate at Talos Dome site (East Antarctica). Sci. Total Environ. 550, 418.

Cole-Dai, J., Ferris, D.G., Lanciki, A.L., Savarino, J., Thiemens, M.H., Mcconnell, J.R., 2013. Two likely stratospheric volcanic eruptions in the 1450s C.E. found in a bipolar, subannually dated 800 year ice core record. J. Geophys. Res. 118, 7459-7466.

Cole-Dai, J., Mosley-Thompson, E., Thompson, L.G., 1997. Annually resolved southern hemisphere volcanic history from two Antarctic ice cores. J. Geophys. Res. 102, 16761 – 16771.

Cole-Dai, J., Mosley-Thompson, E., Wight, S.P., Thompson, L.G., 2000. A 4100-year record of explosive volcanism from an East Antarctica ice core. J. Geophys. Res. 105, 24431-24442.

Cunningham, J., Waddington, E., 1993. Air flow and dry deposition of non-sea salt sulfate in polar firn: paleoclimatic implications. Atmospheric Environment. Part A. General Topics 27, 2943-2956.

Das, I., Bell, R.E., Scambos, T.A., Wolovick, M., Creyts, T.T., Studinger, M., Frearson, N., Nicolas, J.P., Lenaerts, J.T., van den Broeke, M.R., 2013. Influence of persistent wind scour on the surface mass balance of Antarctica. Nat. Geosci. 6, 367-371.

Delmas, R., 1992. Environmental information from ice cores. Rev. Geophys. 30, 1-21.

Delmonte, B., Baroni, C., Andersson, P., Narcisi, B., Salvatore, M.C., Petit, J., Scarchilli, C., Frezzotti, M., Albani, S., Maggi, V., 2013. Modern and Holocene aeolian dust variability from Talos Dome (Northern Victoria Land) to the interior of the Antarctic ice sheet. Quaternary Sci. Rev. 64, 76-89.

Ding, M., Xiao, C., Li, C., Qin, D., Jin, B., Shi, G., Xie, A., Cui, X., 2015. Surface mass balance and its climate significance from the coast to Dome A, East Antarctica. Science China Earth Sciences 58, 1787-1797.

Ding, M., Xiao, C., Li, Y., Ren, J., Hou, S., Jin, B., Sun, B., 2011. Spatial variability of surface mass balance along a traverse route from Zhongshan station to Dome A, Antarctica. J. Glaciol. 57, 658-666.

Ding, M., Xiao, C., Yang, Y., Wang, Y., Li, C., Yuan, N., Shi, G., Sun, W., Ming, J., 2016. Re-assessment of recent (2008–2013) surface mass balance over Dome Argus, Antarctica. Polar Res. 35, 26133.

Dixon, D.A., Mayewski, P.A., Korotkikh, E., Sneed, S.B., Handley, M.J., Introne, D.S., Scambos, T.A., 2013. Variations in snow and firn chemistry along US ITASE traverses and the effect of surface glazing. Cryosphere 7, 515-535.

Du, Z., Xiao, C., Ding, M., Li, C., 2018. Identification of multiple natural and anthropogenic sources of dust in snow from Zhongshan Station to Dome A, East Antarctica. J. Glaciol. 64, 855-865.

Du, Z., Xiao, C., Handley, M.J., Mayewski, P.A., Li, C., Liu, S., Ma, X., Yang, J., 2019. Fe variation

796 characteristics and sources in snow samples along a traverse from Zhongshan Station to Dome A, East
797 Antarctica. Sci. Total Environ.
798 EPICA Community Members, 2004. Eight glacial cycles from an Antarctic ice core. Nature 429,
799 623-628.
800 Erbland, J., Vicars, W., Savarino, J., Morin, S., Frey, M., Frosini, D., Vince, E., Martins, J., 2013.
801 Air-snow transfer of nitrate on the East Antarctic Plateau - Part 1: Isotopic evidence for a photolytically
802 driven dynamic equilibrium in summer. Atmos. Chem. Phys. 13, 6403-6419.
803 Finlayson-Pitts, B.J., 2003. The tropospheric chemistry of sea salt: a molecular-level view of the
804 chemistry of NaCl and NaBr. Chem. Rev. 103, 4801-4822.
805 Frey, M.M., Norris, S.J., Brooks, I.M., Anderson, P.S., Nishimura, K., Yang, X., Jones, A.E., Nerentorp
806 Mastromonaco, M.G., Jones, D.H., Wolff, E.W., 2020. First direct observation of sea salt aerosol
807 production from blowing snow above sea ice. Atmos. Chem. Phys. 20, 2549-2578.
808 Goodwin, I., Van Ommen, T., Curran, M., Mayewski, P., 2004. Mid latitude winter climate variability
809 in the South Indian and southwest Pacific regions since 1300 AD. Clim. Dynam. 22, 783-794.
810 Gragnani, R., Smiraglia, C., Stenni, B., Torcini, S., 1998. Chemical and isotopic profiles from snow
811 pits and shallow firn cores on Campbell Glacier, northern Victoria Land, Antarctica. Ann. Glaciol. 27,
812 679-684.
813 Hara, K., Nakazawa, F., Fujita, S., Fukui, K., Enomoto, H., Sugiyama, S., 2014. Horizontal
814 distributions of aerosol constituents and their mixing states in Antarctica during the JASE traverse.
815 Atmos. Chem. Phys. 14, 10211-10230.
816 Hara, K., Osada, K., Yamanouchi, T., 2013. Tethered balloon-borne aerosol measurements: seasonal
817 and vertical variations of aerosol constituents over Syowa Station, Antarctica. Atmos. Chem. Phys. 13,
818 9119-9139.
819 Holland, P.R., Bruneau, N., Enright, C., Losch, M., Kurtz, N.T., Kwok, R., 2014. Modeled Trends in
820 Antarctic Sea Ice Thickness. J. Climate 27, 3784-3801.
821 Hou, S., Li, Y., Xiao, C., Ren, J., 2007. Recent accumulation rate at Dome A, Antarctica. Chin. Sci.
822 Bull. 52, 428-431.
823 Ishino, S., Hattori, S., Savarino, J., Jourdain, B., Preunkert, S., Legrand, M., Caillon, N., Barbero, A.,
824 Kuribayashi, K., Yoshida, N., 2017. Seasonal variations of triple oxygen isotopic compositions of
825 atmospheric sulfate, nitrate and ozone at Dumont d'Urville, coastal Antarctica. Atmos. Chem. Phys. 17,
826 1-25.
827 Jiang, S., Cole-Dai, J., Li, Y., Ferris, D.G., Ma, H., An, C., Shi, G., Sun, B., 2012. A detailed 2840 year
828 record of explosive volcanism in a shallow ice core from Dome A, East Antarctica. J. Glaciol. 58,
829 65-75.
830 Johnson, M., Sanders, R., Avgoustidi, V., Lucas, M., Brown, L., Hansell, D., Moore, M., Gibb, S., Liss,
831 P., Jickells, T., 2007. Ammonium accumulation during a silicate-limited diatom bloom indicates the
832 potential for ammonia emission events. Mar. Chem. 106, 63-75.
833 Jouzel, J., Masson-Delmotte, V., Cattani, O., Dreyfus, G., Falourd, S., Hoffmann, G., Minster, B.,
834 Nouet, J., Barnola, J.M., Chappellaz, J., Fischer, H., Gallet, J.C., Johnsen, S., Leuenberger, M.,
835 Loulergue, L., Luethi, D., Oerter, H., Parrenin, F., Raisbeck, G., Raynaud, D., Schilt, A., Schwander, J.,
836 Selmo, E., Souchez, R., Spahni, R., Stauffer, B., Steffensen, J.P., Stenni, B., Stocker, T.F., Tison, J.L.,
837 Werner, M., Wolff, E.W., 2007. Orbital and Millennial Antarctic Climate Variability over the Past
838 800,000 Years. Science 317, 793-796.
839 Kärkäs, E., Teinilä, K., Virkkula, A., Aurela, M., 2005. Spatial variations of surface snow chemistry

during two austral summers in western Dronning Maud Land, Antarctica. Atmos. Environ. 39, 1405-1416.
Kaufmann, P., Fundel, F., Fischer, H., Bigler, M., Ruth, U., Udisti, R., Hansson, M., De Angelis, M., Barbante, C., Wolff, E.W., 2010. Ammonium and non-sea salt sulfate in the EPICA ice cores as indicator of biological activity in the Southern Ocean. Quaternary Sci. Rev. 29, 313-323.
Keene, W.C., Maring, H., Maben, J.R., Kieber, D.J., Pszenny, A.A., Dahl, E.E., Izaguirre, M.A., Davis, A.J., Long, M.S., Zhou, X., 2007. Chemical and physical characteristics of nascent aerosols produced by bursting bubbles at a model air - sea interface. J. Geophys. Res. 112. D21202.
Khodzher, T.V., Golobokova, L.P., Osipov, E.Y., Shibaev, Y.A., Lipenkov, V.Y., Osipova, O.P., Petit, J.R., 2014. Spatial-temporal dynamics of chemical composition of surface snow in East Antarctica along the Progress station-Vostok station transect. Cryosphere 8, 931–939.
Krinner, G., Genthon, C., 2003. Tropospheric transport of continental tracers towards Antarctica under varying climatic conditions. Tellus B 55, 54-70.
Krinner, G., Petit, J.R., Delmonte, B., 2010. Altitude of atmospheric tracer transport towards Antarctica inpresent and glacial climate. Quaternary Sci. Rev. 29, 274-284.
Lee, H.-M., Henze, D.K., Alexander, B., Murray, L.T., 2014. Investigating the sensitivity of surface-level nitrate seasonality in Antarctica to primary sources using a global model. Atmos. Environ. 89, 757-767.
Legrand, M., 1987. Chemistry of Antarctic snow and ice. J. de Phys. 48, 77-86.
Legrand, M., 1995. Sulphur-derived species in polar ice: a review, in: Delmas, R. (Ed.), Ice core studies of global biogeochemical cycles. Springer, pp. 91-119.
Legrand, M., 1997. Ice–core records of atmospheric sulphur. Phil. Trans. R. Soc. Lond. B 352, 241-250.
Legrand, M., Delmas, R., 1987. A 220-year continuous record of volcanic H_2SO_4 in the Antarctic ice sheet. Nature 327, 671-676.
Legrand, M., Delmas, R.J., 1985. Spatial and temporal variations of snow chemistry in Terre Adélie (East Antarctica). Ann. Glaciol. 7, 20-25.
Legrand, M., Ducroz, F., Wagenbach, D., Mulvaney, R., Hall, J., 1998. Ammonium in coastal Antarctic aerosol and snow: Role of polar ocean and penguin emissions. J. Geophys. Res. 103, 11043-11056.
Legrand, M., Lorius, C., Barkov, N., Petrov, V., 1988. Vostok (Antarctica) ice core: Atmospheric chemistry changes over the last climatic cycle (160,000 years). Atmos. Environ. 22, 317-331.
Legrand, M., Mayewski, P.A., 1997. Glaciochemistry of polar ice cores: a review. Rev. Geophys. 35, 219-243.
Legrand, M., Preunkert, S., Weller, R., Zipf, L., Elsässer, C., Merchel, S., Rugel, G., Wagenbach, D., 2017a. Year-round record of bulk and size-segregated aerosol composition in central Antarctica (Concordia site) – Part 2: Biogenic sulfur (sulfate and methanesulfonate) aerosol. Atmos. Chem. Phys. 17, 14055-14073.
Legrand, M., Preunkert, S., Wolff, E., Weller, R., Jourdain, B., Wagenbach, D., 2017b. Year-round records of bulk and size-segregated aerosol composition in central Antarctica (Concordia site) – Part 1: Fractionation of sea-salt particles. Atmos. Chem. Phys. 17, 14039-14054.
Legrand, M., Wolff, E., Wagenbach, D., 1999. Antarctic aerosol and snowfall chemistry: implications for deep Antarctic ice-core chemistry. Ann. Glaciol. 29, 66-72.
Legrand, M., Yang, X., Preunkert, S., Theys, N., 2016. Year-round records of sea salt, gaseous, and particulate inorganic bromine in the atmospheric boundary layer at coastal (Dumont d'Urville) and

884 central (Concordia) East Antarctic sites. J. Geophys. Res. 121, 2015JD024066.
885 Legrand, M.R., Delmas, R.J., 1984. The ionic balance of Antarctic snow: a 10-year detailed record.
886 Atmos. Environ. 18, 1867-1874.
887 Levine, J., Yang, X., Jones, A., Wolff, E., 2014. Sea salt as an ice core proxy for past sea ice extent: A
888 process‐based model study. J. Geophys. Res. 119, 5737-5756.
889 Li, C., Xiao, C., Shi, G., Ding, M., Kang, S., Zhang, L., Hou, S., Sun, B., Qin, D., Ren, J., 2015.
890 Spatiotemporal variations of monocarboxylic acids in snow layers along a transect from Zhongshan
891 Station to Dome A, eastern Antarctica. Atmos. Res. 158-159, 79-87.
892 Li, C., Xiao, C., Shi, G., Ding, M., Qin, D., Ren, J., 2016. Spatial and temporal variability of
893 marine-origin matter along a transect from Zhongshan Station to Dome A, Eastern Antarctica. J.
894 Environ. Sci. 46, 190-202.
895 Libois, Q., Picard, G., Arnaud, L., Morin, S., Brun, E., 2014. Modeling the impact of snow drift on the
896 decameter‐scale variability of snow properties on the Antarctic Plateau. J. Geophys. Res. 119,
897 11,662-611,681.
898 Ma, X., Li, C., Du, Z., Dou, T., Ding, M., Ming, J., Wang, M., Gao, S., Xiao, C., Wang, X., Ren, J.,
899 Kang, S., 2020. Spatial and temporal variations of refractory black carbon along the transect from
900 Zhongshan Station to Dome A, eastern Antarctica. Atmos. Environ., 117816.
901 Mahalinganathan, K., Thamban, M., 2016. Potential genesis and implications of calcium nitrate in
902 Antarctic snow. Cryosphere 10, 825-836.
903 Mahalinganathan, K., Thamban, M., Laluraj, C.M., Redkar, B.L., 2011. Relation between surface
904 topography and sea-salt snow chemistry from Princess Elizabeth Land, East Antarctica. Cryosphere 6,
905 505-515.
906 Marion, G., Farren, R., Komrowski, A., 1999. Alternative pathways for seawater freezing. Cold Reg.
907 Sci. Technol. 29, 259-266.
908 Mayewski, P.A., Carleton, A.M., Birkel, S.D., Dixon, D., Kurbatov, A.V., Korotkikh, E., McConnell, J.,
909 Curran, M., Cole-Dai, J., Jiang, S., Plummer, C., Vance, T., Maasch, K.A., Sneed, S.B., Handley, M.,
910 2017. Ice core and climate reanalysis analogs to predict Antarctic and Southern Hemisphere climate
911 changes. Quaternary Sci. Rev. 155, 50-66.
912 Mulvaney, R., Wolff, E., 1994. Spatial variability of the major chemistry of the Antarctic ice sheet. Ann.
913 Glaciol. 20, 440-447.
914 Pasteris, D.R., McConnell, J.R., Das, S.B., Criscitiello, A.S., Evans, M.J., Maselli, O.J., Sigl, M.,
915 Layman, L.C.J.D., 2014. Seasonally resolved ice core records from West Antarctica indicate a sea ice
916 source of sea-salt aerosol and a biomass burning source of ammonium. J. Geophys. Res. 119,
917 9168-9182.
918 Pasteris, D.R., Mcconnell, J.R., Edwards, R., 2012. High-resolution, continuous method for
919 measurement of acidity in ice cores. Environ. Sci. Technol. 46, 1659.
920 Proposito, M., Becagli, S., Castellano, E., Flora, O., Genoni, L., Gragnani, R., Stenni, B., Traversi, R.,
921 Udisti, R., Frezzotti, M., 2002. Chemical and isotopic snow variability along the 1998 ITASE traverse
922 from Terra Nova Bay to Dome C, East Antarctica. Ann. Glaciol. 35, 187-194.
923 Qin, D., Zeller, E.J., Dreschhoff, G.A., 1992. The distribution of nitrate content in the surface snow of
924 the Antarctic Ice Sheet along the route of the 1990 International Trans-Antarctica Expedition. J.
925 Geophys. Res. 97, 6277-6284.
926 Röthlisberger, R., Mulvaney, R., Wolff, E.W., Hutterli, M.A., Bigler, M., De Angelis, M., Hansson,
927 M.E., Steffensen, J.P., Udisti, R., 2003. Limited dechlorination of sea-salt aerosols during the last

928 glacial period: Evidence from the European Project for Ice Coring in Antarctica (EPICA) Dome C ice
929 core. J. Geophys. Res. 108, 4526, doi:4510.1029/2003JD003604.
930 Rankin, A.M., Wolff, E.W., 2000. Ammonium and potassium in snow around an emperor penguin
931 colony. Antarct. Sci. 12, 154-159.
932 Russell, A., McGregor, G.R., 2010. Southern hemisphere atmospheric circulation: impacts on Antarctic
933 climate and reconstructions from Antarctic ice core data. Climatic. Change 99, 155-192.
934 Saltzman, E.S., 1995. Ocean/atmosphere cycling of dimethylsulfide, in: Delmas, R.J. (Ed.), Ice core
935 studies of global biogeochemical cycles. Springer, Berlin, pp. 65-89.
936 Sato, K., Takenaka, N., Bandow, H., Maeda, Y., 2008. Evaporation loss of dissolved volatile substances
937 from ice surfaces. J. Phys. Chem. 112, 7600-7607.
938 Savarino, J., Kaiser, J., Morin, S., Sigman, D.M., Thiemens, M.H., 2007. Nitrogen and oxygen isotopic
939 constraints on the origin of atmospheric nitrate in coastal Antarctica. Atmos. Chem. Phys. 7,
940 1925-1945.
941 Severi, M., Becagli, S., Caiazzo, L., Ciardini, V., Colizza, E., Giardi, F., Mezgec, K., Scarchilli, C.,
942 Stenni, B., Thomas, E.R., Traversi, R., Udisti, R., 2017. Sea salt sodium record from Talos Dome (East
943 Antarctica) as a potential proxy of the Antarctic past sea ice extent. Chemosphere 177, 266-274.
944 Severi, M., Becagli, S., Castellano, E., Morganti, A., Traversi, R., Udisti, R., 2009. Thirty years of
945 snow deposition at Talos Dome (Northern Victoria Land, East Antarctica): Chemical profiles and
946 climatic implications. Microchem. J. 92, 15-20.
947 Shi, G., Buffen, A.M., Hastings, M.G., Li, C., Ma, H., Li, Y., Sun, B., An, C., Jiang, S., 2015.
948 Investigation of post-depositional processing of nitrate in East Antarctic snow: isotopic constraints on
949 photolytic loss, re-oxidation, and source inputs. Atmos. Chem. Phys. 15, 9435–9453.
950 Shi, G., Buffen, A.M., Ma, H., Hu, Z., Sun, B., Li, C., Yu, J., Ma, T., An, C., Jiang, S., Li, Y., Hastings,
951 M.G., 2018a. Distinguishing summertime atmospheric production of nitrate across the East Antarctic
952 Ice Sheet. Geochim. Cosmochim. Acta 231, 1-14.
953 Shi, G., Hastings, M.G., Yu, J., Ma, T., Hu, Z., An, C., Li, C., Ma, H., Jiang, S., Li, Y., 2018b. Nitrate
954 deposition and preservation in the snowpack along a traverse from coast to the ice sheet summit (Dome
955 A) in East Antarctica. The Cryosphere 12, 1177–1194.
956 Shi, G., Li, Y., Jiang, S., An, C., Ma, H., Sun, B., Wang, Y., 2012. Large-scale spatial variability of
957 major ions in the atmospheric wet deposition along the China Antarctica transect (31^{o} N~ 69^{o} S). Tellus
958 B 64, 17134.
959 Shi, G., Wang, X.-C., Li, Y., Trengove, R., Hu, Z., Mi, M., Li, X., Yu, J., Hunter, B., He, T., 2019.
960 Organic tracers from biomass burning in snow from the coast to the ice sheet summit of East Antarctica.
961 Atmos. Environ. 201, 231-241.
962 Sigl, M., Fudge, T.J., Winstrup, M., Cole-Dai, J., Ferris, D., Mcconnell, J.R., Taylor, K.C., Welten, K.C.,
963 Woodruff, T.E., Adolphi, F., Bisiaux, M., Brook, E.J., Buizert, C., Caffee, M.W., Dunbar, N.W.,
964 Edwards, R., Geng, L., Iverson, N., Koffman, B., Layman, L., Maselli, O.J., McGwire, K., Muscheler,
965 R., Nishiizumi, K., Pasteris, D.R., Rhodes, R.H., Sowers, T.A., 2016. The WAIS Divide deep ice core
966 WD2014 chronology - Part 2: Annual-layer counting (0-31 ka BP). Clim. Past 12, 769-786.
967 Suzuki, T., Iizuka, Y., Matsuoka, K., Furukawa, T., Kamiyama, K., Watanabe, O., 2002. Distribution of
968 sea salt components in snow cover along the traverse route from the coast to Dome Fuji station 1000
969 km inland at east Dronning Maud Land, Antarctica. Tellus B Chemical and Physical Meteorology 54,
970 407-411.
971 Traversi, R., Becagli, S., Castellano, E., Cerri, O., Morganti, A., Severi, M., Udisti, R., 2009. Study of

Dome C site (East Antartica) variability by comparing chemical stratigraphies. Microchem. J. 92, 7-14.
Traversi, R., Becagli, S., Castellano, E., Largiuni, O., Migliori, A., Severi, M., Frezzotti, M., Udisti, R., 2004. Spatial and temporal distribution of environmental markers from Coastal to Plateau areas in Antarctica by firn core chemical analysis. Int. J. Environ. Anal. Chem. 84, 457-470.
Udisti, R., Becagli, S., Benassai, S., Castellano, E., Fattori, I., Innocenti, M., Migliori, A., Traversi, R., 2004. Atmosphere-snow interaction by a comparison between aerosol and uppermost snow layers composition at Dome Concordia (East Antarctica). Ann. Glaciol. 39, 53-61(59).
Udisti, R., Dayan, U., Becagli, S., Busetto, M., Frosini, D., Legrand, M., Lucarelli, F., Preunkert, S., Severi, M., Traversi, R., 2012. Sea spray aerosol in central Antarctica. Present atmospheric behaviour and implications for paleoclimatic reconstructions. Atmos. Environ. 52, 109-120.
Virkkula, A., Teinilä, K., Hillamo, R., Kerminen, V.M., Saarikoski, S., Aurela, M., Koponen, I.K., Kulmala, M., 2006. Chemical size distributions of boundary layer aerosol over the Atlantic Ocean and at an Antarctic site. Atmos. Chem. Phys. 6, 303-310.
Wagenbach, D., 1996. Coastal Antarctica: Atmospheric chemical composition and atmospheric transport, in: Wolff, E.W., Bales, R.C. (Eds.), Chemical Exchange between the Atmosphere and polar snow. Springer-Verlag, New York, pp. 173-199.
Wagenbach, D., Ducroz, F., Mulvaney, R., Keck, L., Minikin, A., Legrand, M., Hall, J.S., Wolff, E.W., 1998a. Sea-salt aerosol in coastal Antarctic regions. J. Geophys. Res. 103, 10961-10974.
Wagenbach, D., Legrand, M., Fischer, H., Pichlmayer, F., Wolff, E.W., 1998b. Atmospheric near-surface nitrate at coastal Antarctic sites. J. Geophys. Res. 103, 11007-11020.
Wagnon, P., Delmas, R.J., Legrand, M., 1999. Loss of volatile acid species from the upper firn layers at Vostok, Antarctica. J. Geophys. Res. 104, 3423-3431.
Weller, R., Wagenbach, D., Legrand, M., Elsässer, C., Tian-kunze, X., Königlanglo, G., 2011. Continuous 25-yr aerosol records at coastal Antarctica-: inter-annual variability of ionic compounds and links to climate indices. Tellus B 63, 901-919.
Wolff, E.W., Barbante, S., Becagle, S., Bigler, M., Boutron, C.F., Castellano, E., de Angelis, M., Federer, U., 2010. Changes in environment over the last 800,000 years from chemical analysis of the EPICA Dome C ice core. Quaternary Sci. Rev. 29, 285-295.
Wolff, E.W., Fischer, H., Fundel, F., Ruth, U., Twarloh, B., Littot, G.C., Mulvaney, R., Röthlisberger, R., de Angelis, M., Boutron, C.F., Hansson, M., Jonsell, U., Hutterli, M.A., Lambert, F., Kaufmann, P., Stauffer, B., Stocker, T.F., Steffensen, J.P., Bigler, M., Siggaard-Andersen, M.L., Udisti, R., Becagli, S., Castellano, E., Severi, M., Wagenbach, D., Barbante, C., Gabrielli, P., Gaspari, V., 2006. Southern Ocean sea-ice extent, productivity and iron flux over the past eight glacial cycles. Nature 440, 491-496.
Wolff, E.W., Rankin, A.M., Röthlisberger, R., 2003. An ice core indicator of Antarctic sea ice production? Geophys. Res. Lett. 30, doi:10.1029/2003GL018454.
Zhao, L., Moore, J.C., Sun, B., Tang, X., Guo, X., 2018. Where is the 1-million-year-old ice at Dome A? The Cryosphere 12, 1651–1663.

Table 1 Rotated component matrix of the major ions in surface snow. (Extraction method: principal component analysis. Rotation method: varimax with Kaiser normalization. Rotation converged in 4 iterations.) Factor loadings were calculated from the eigenvalues of the three components and their corresponding eigenvectors, and the values greater than 0.7 are shaded.

Chemical ions	PC1	PC2	PC3	Communalities
Cl^-	0.93	-0.01	0.27	0.93
NO_3^-	0.04	-0.06	0.95	0.90
SO_4^{2-}	0.55	0.08	0.42	0.49
Na^+	0.98	-0.01	-0.06	0.96
NH_4^+	0.10	0.81	0.04	0.66
K^+	0.71	0.25	0.12	0.57
Mg^{2+}	0.96	0.05	-0.09	0.92
Ca^{2+}	0.03	0.79	-0.07	0.62
Initial eigenvalues	3.67	1.33	1.06	
Percentage of variance	46	17	13	
Cumulative percent	46	63	76	

Table 2 Pearson correlation matrix of major ions in surface snow

	Cl^-	NO_3^-	SO_4^{2-}	Na^+	NH_4^+	K^+	Mg^{2+}	Ca^{2+}
Cl^-	1.00	0.24**	0.47**	0.94**	0.05	0.74**	0.91**	0.09
NO_3^-		1.00	0.21**	-0.02	-0.04	0.09*	-0.04	-0.05
SO_4^{2-}			1.00	0.34**	0.08	0.30**	0.31**	0.03
Na^+				1.00	0.05	0.77**	0.98**	0.12*
NH_4^+					1.00	0.19**	0.10*	0.30**
K^+						1.00	0.75**	0.15**
Mg^{2+}							1.00	0.15**
Ca^{2+}								1.00

**. Correlation is significant at the 0.01 level (2-tailed).

*. Correlation is significant at the 0.05 level (2-tailed).

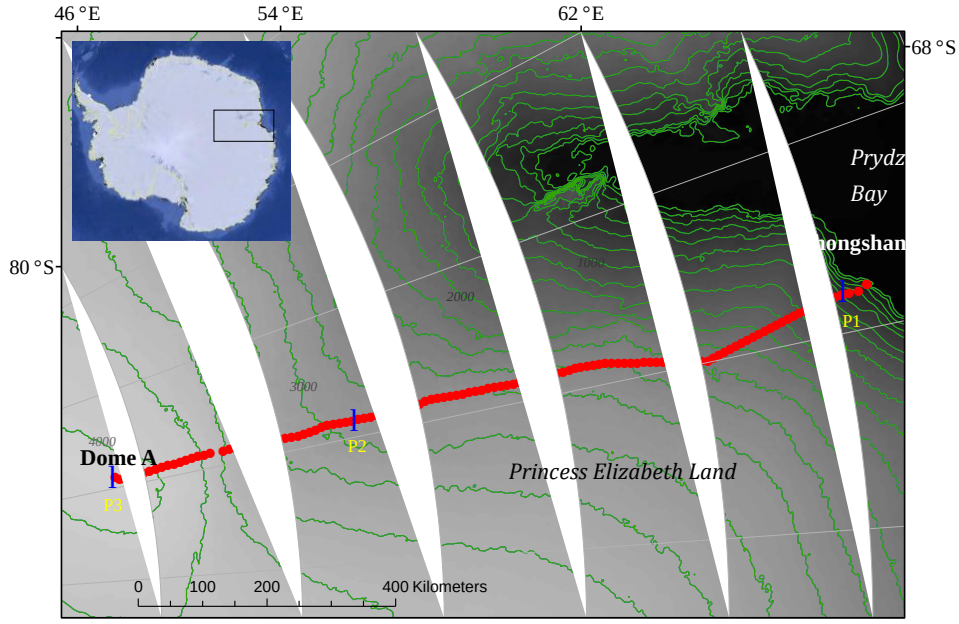

Figure 1. The Chinese inland investigation traverse from the coast (Zhongshan station) to the ice sheet summit, Dome A, East Antarctica. The traverse is generally along the 77.0 °E longitude.

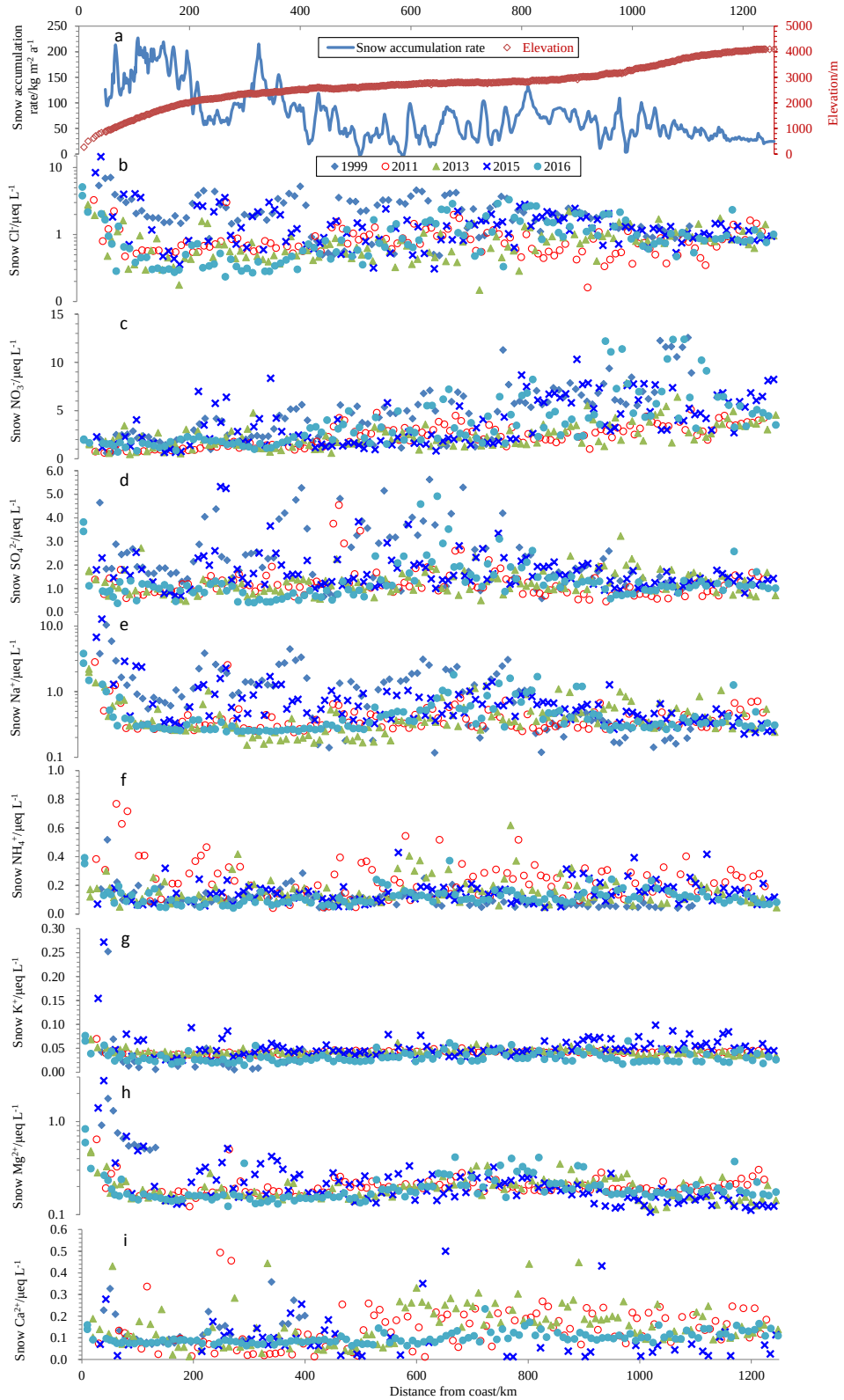
a
Snow accumulation rate
Elevation
Snow accumulation rate/kg m^{-2} a^{-1}
Elevation/m
b
1999
2011
2013
2015
2016
Snow Cl$^-$/μeq L^{-1}
c
Snow NO$_3^-$/μeq L^{-1}
d
Snow SO$_4^{2-}$/μeq L^{-1}
e
Snow Na$^+$/μeq L^{-1}
f
Snow NH$_4^+$/μeq L^{-1}
g
Snow K$^+$/μeq L^{-1}
h
Snow Mg^{2+}/μeq L^{-1}
i
Snow Ca^{2+}/μeq L^{-1}
Distance from coast/km

1028

Figure 2. Annual snow accumulation rate, elevation (a) and ion concentrations in surface snow collected during five seasons (b-i). Annual snow accumulation rate is obtained from field bamboo stick measurements, updated to 2016 from Ding et al. (2011). The closed diamond, open circle, closed triangle, cross and closed circle denote ion concentrations in the years 1999, 2011, 2013, 2015, and 2016, respectively. Note that a base-10 log scale is used for the *y*-axis of Cl^- (b), Na^+ (e), and Mg^{2+} (h).

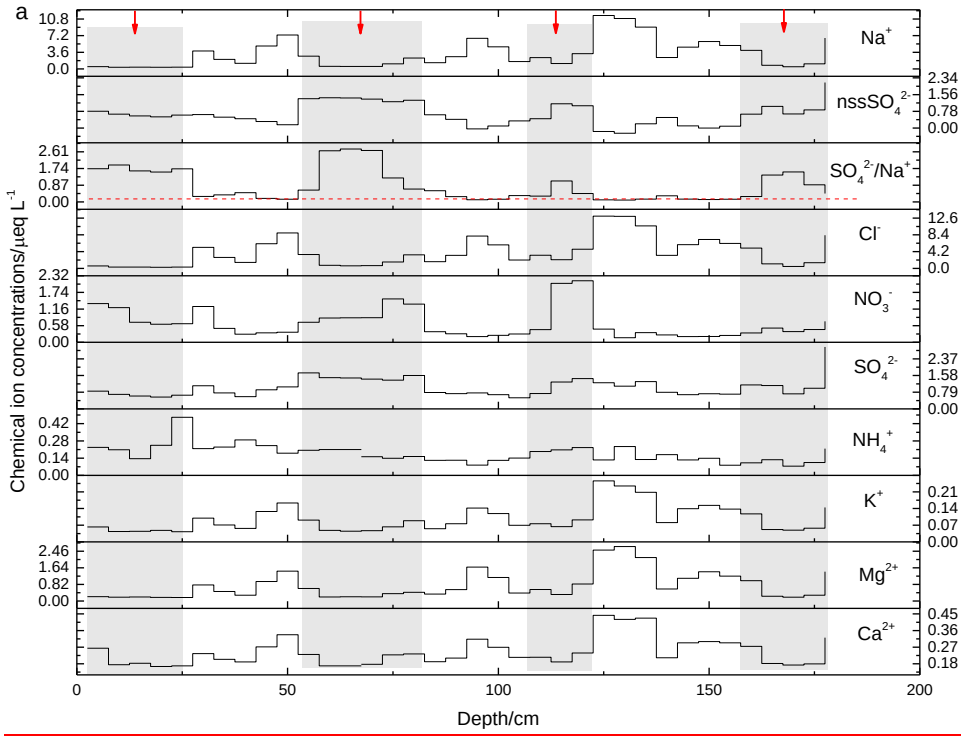
a
Chemical ion concentrations/μeq L-1
Na+
nssSO4 2-
SO4 2-/Na+
Cl-
NO3-
SO4 2-
NH4+
K+
Mg2+
Ca2+
Depth/cm

1035

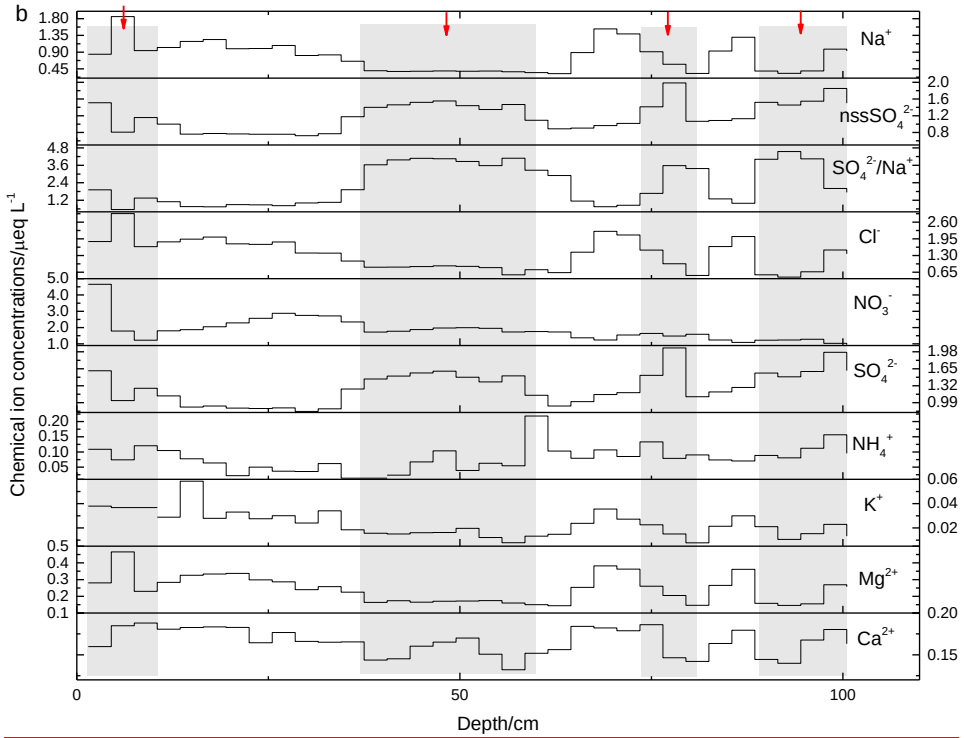
b
Chemical ion concentrations/μeq L-1
Na+
nssSO4 2-
SO4 2-/Na+
Cl-
NO3-
SO4 2-
NH4+
K+
Mg2+
Ca2+
Depth/cm

1036

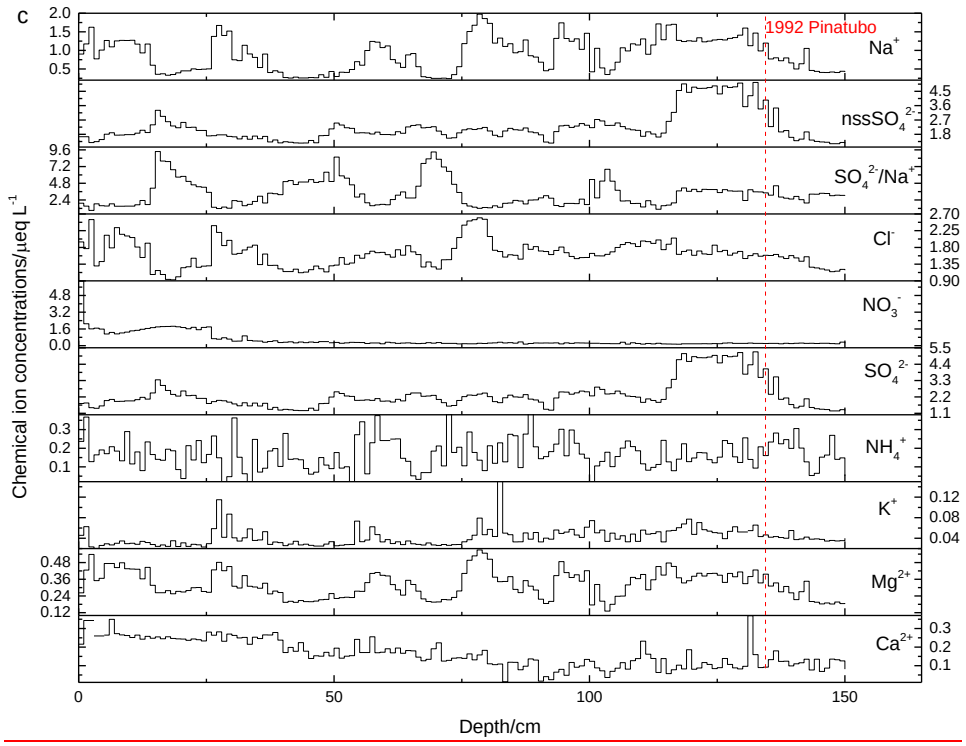

Figure 3. Profiles of chemical ions in snow pits P1 (a), P2 (b), and P3 (c). Snow pits P1 and P2 were sampled in the summer season in 2015-2016, and P3 was sampled in January 2010. The ratios of SO_4^{2-}/Na^+ in snow samples were also present. Red arrows in panels (a) and (b) represent the middle of the identified summer, and shaded areas denote summer seasons (see text). The red dashed line in panel (a) represents the ratio of SO_4^{2-}/Na^+ in bulk seawater, while the red dashed line in panel (c) signifies the first snow sample significantly influenced by the Pinatubo eruption. One seasonal cycle generally represents local Na^+ minima and $nssSO_4^{2-}$ and SO_4^{2-}/Na^+ maxima.

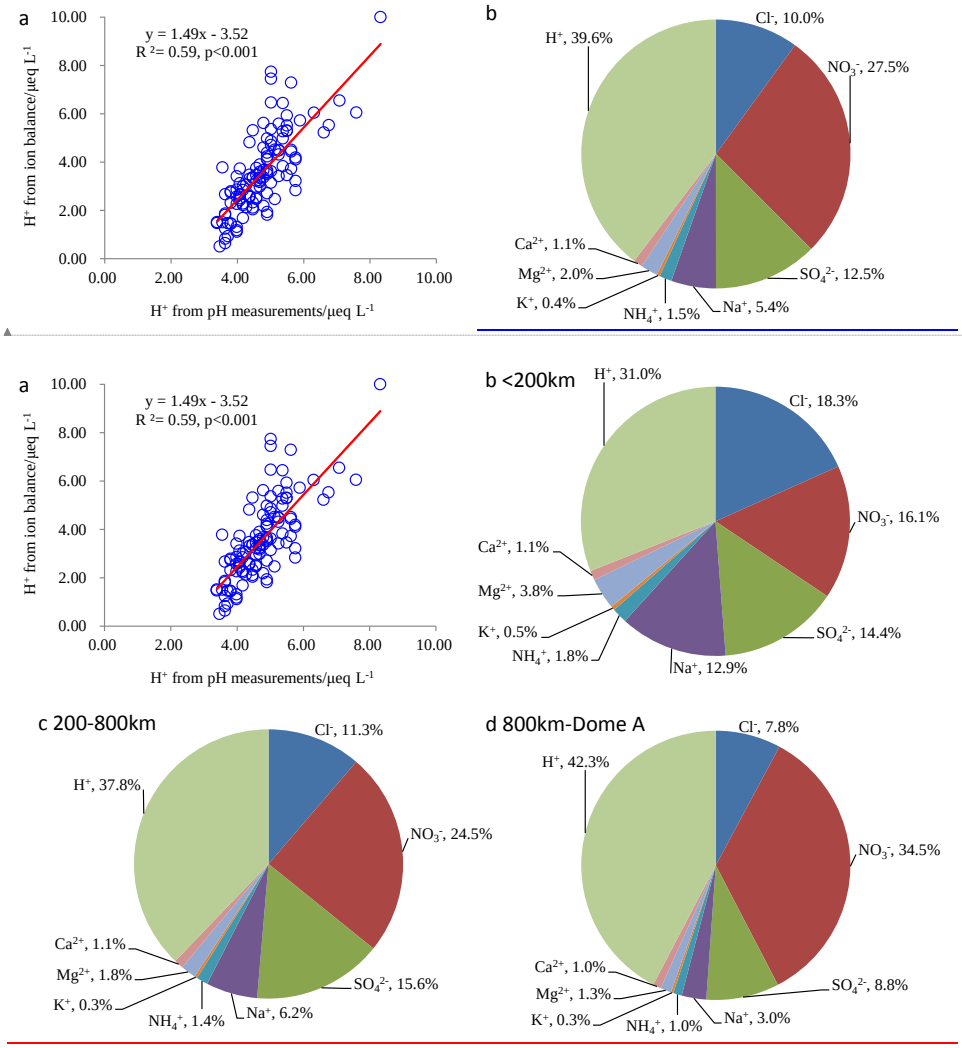

Figure 34. Major ions in surface snow on the Chinese inland Antarctic traverse. Concentrations of H^+ derived from pH versus those from the ion balance method are shown in panel (a), and contribution percentages of each ion to the total in different regions on the traverse are shown in panels (b)-(d), in μeq L^{-1}. The percentages of each ion in individual regions were calculated from the averages of all sites within the region.

带格式的：字体：10 磅

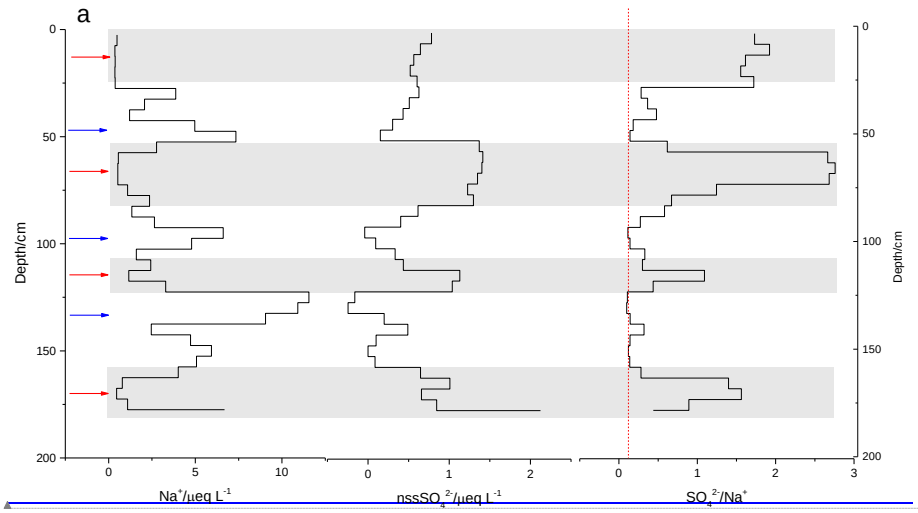

1056

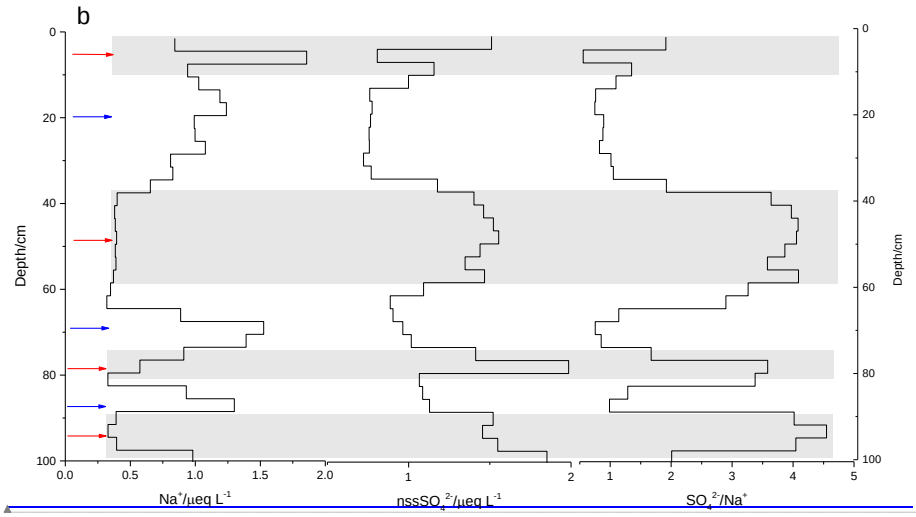

1057

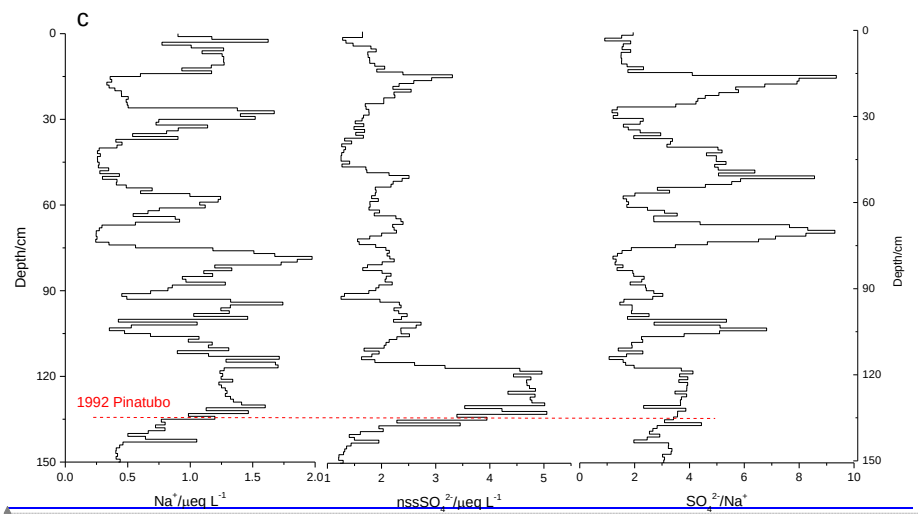

1058

带格式的：字体：10 磅

带格式的：字体：10 磅

带格式的：字体：10 磅

~~**Figure 4.** Profiles of SO_4^{2-}, Na^+, and SO_4^{2-}/Na^+ ratios in snow pits P1 (a), P2 (b), and P3 (c). Red and blue arrows in panels (a) and (b) represent the middle of the identified summer and winter seasons, respectively, and shaded areas denote summer seasons (see text). The red dashed line in panel (a) represents the ratio of SO_4^{2-}/Na^+ in bulk seawater, while the red dashed line in panel (c) signifies the first snow sample significantly influenced by the Pinatubo eruption. One seasonal cycle generally represents local Na^+ minima and $nssSO_4^{2-}$ and SO_4^{2-}/Na^+ maxima.~~

带格式的：两端对齐，定义网格后不调整右缩进，无孤行控制，不调整西文与中文之间的空格，不调整中文和数字之间的空格

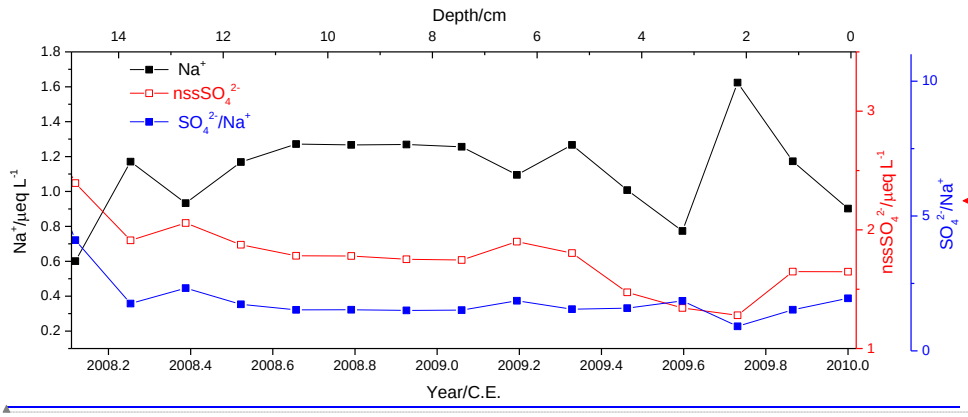

Figure 5. Variations in Na^+, $nssSO_4^{2-}$, and SO_4^{2-}/Na^+ ratio in the snow in the years 2008 and 2009, in Dome A snow pit (P3).

带格式的：两端对齐，缩进：首行缩进： 0 字符，定义网格后不调整右缩进，无孤行控制，不调整西文与中文之间的空格，不调整中文和数字之间的空格

带格式的：字体：10 磅

带格式的：定义网格后不调整右缩进，不调整西文与中文之间的空格，不调整中文和数字之间的空格

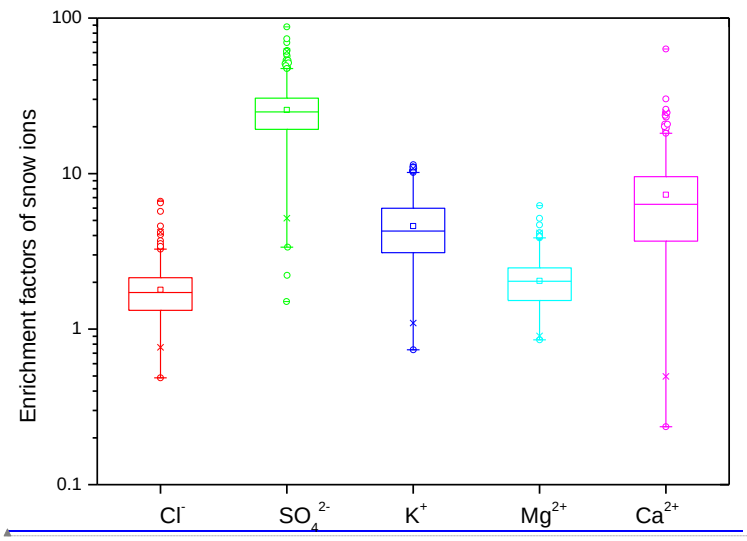

带格式的：字体：10 磅

Figure 6. Statistics of enrichment factors of ions in surface snow. Box-and-whisker plots represent maximum (top end dash symbol for each box), minimum (bottom end dash symbol for each box), the range 1-99 % (top and bottom X symbol for each box), percentiles (5th, 25th, 75th, and 95th), and median (50th, solid line) and mean (open square near the center of each box). Note that the data outside the range 5-95 % are shown as open circles.

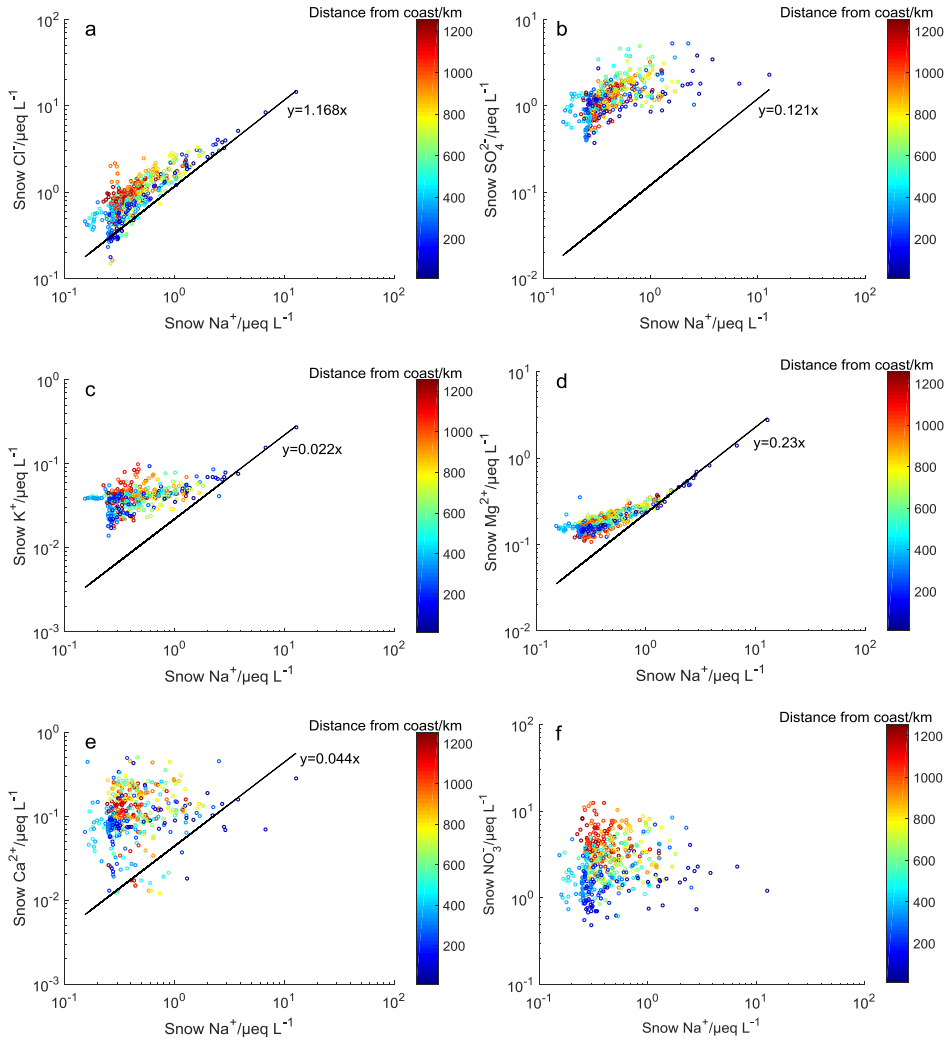

Figure ~~7~~5. Correlation plots of Cl^-, SO_4^{2-}, K^+, Mg^{2+}, Ca^{2+}, and NO_3^- versus Na^+ in surface snow. The black solid line represents the seawater dilution line, with slopes of typical ions versus Na^+ ratios in seawater (in μeq L^{-1}). The concentration of NO_3^- in seawater is too variable among the seas, and a representative ratio of NO_3^-/Na^+ cannot be presented. Note that a base-10 log scale is used for ion concentrations.

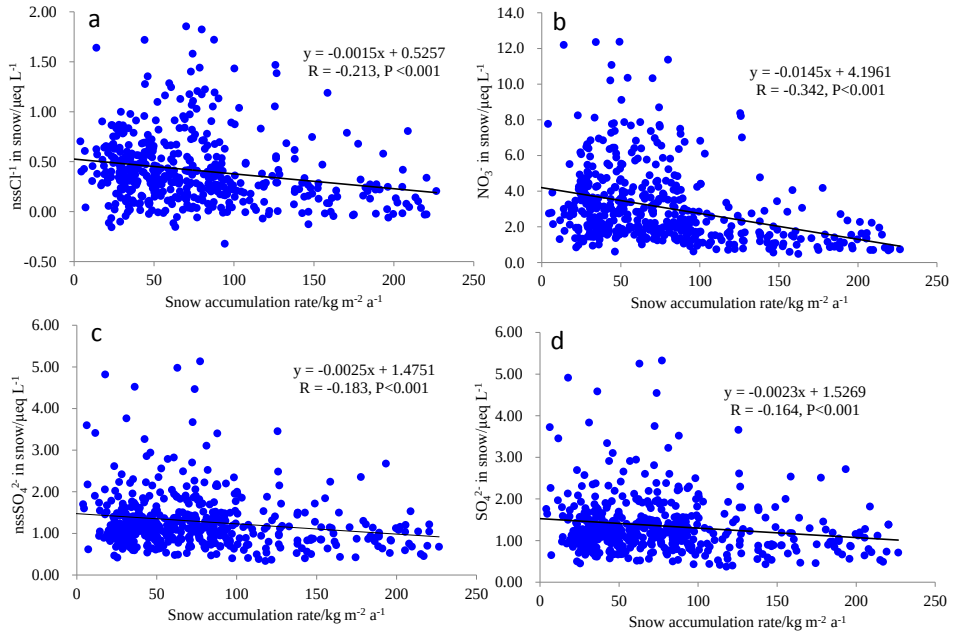

Figure 86. Relationship between chemical ions in surface snow and snow accumulation rate on the traverse.

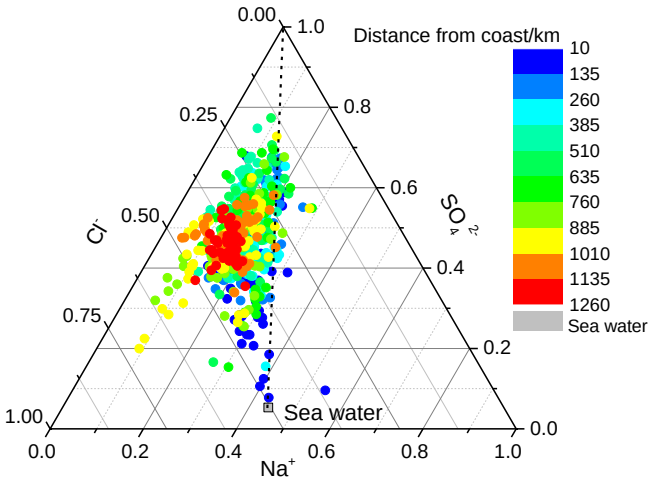

Figure ~~9~~7. Ternary plot of Cl^-, Na^+, and SO_4^{2-} in surface snow samples. Bulk seawater composition is denoted by a grey square. The dashed line extending between the sea salt reference value and the SO_4^{2-} summit represents the composition of sea salt with increasing SO_4^{2-}.

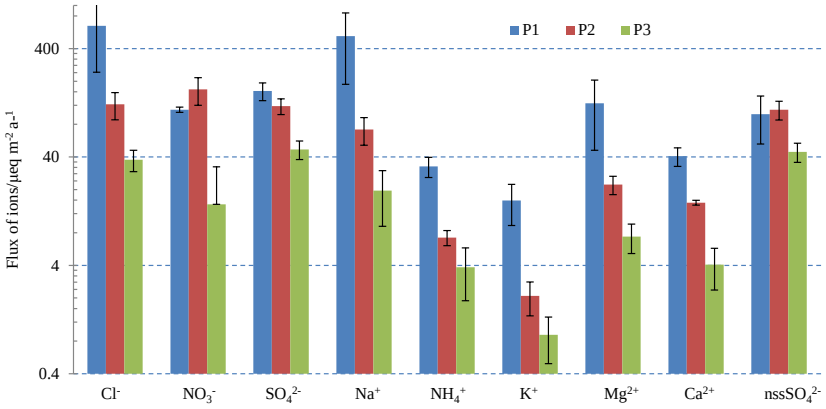

Figure ~~10~~8. Ion fluxes at the three pits (P1, P2, and P3). The error bars represent one standard deviation of fluxes in different years. Note that a base-10 log scale is used for the *y*-axis.

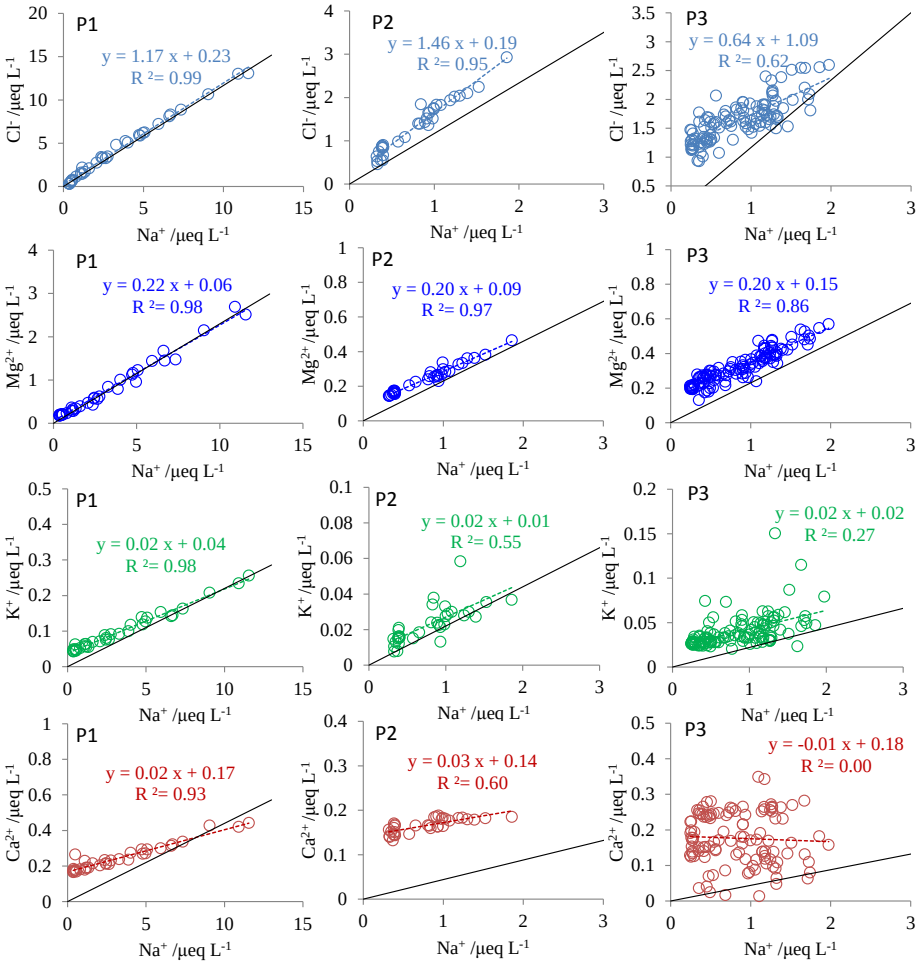

Figure ~~11~~9. Relationships between Na^+ and Cl^-, K^+, Mg^{2+}, Ca^{2+} in the three snow pits (P1, P2, and P3). Also shown are the linear regressions between them (dashed line), with all of the linear correlation significant at $p<0.001$ except Ca^{2+}/Na^+ at P3. The black solid line represents seawater dilution line.

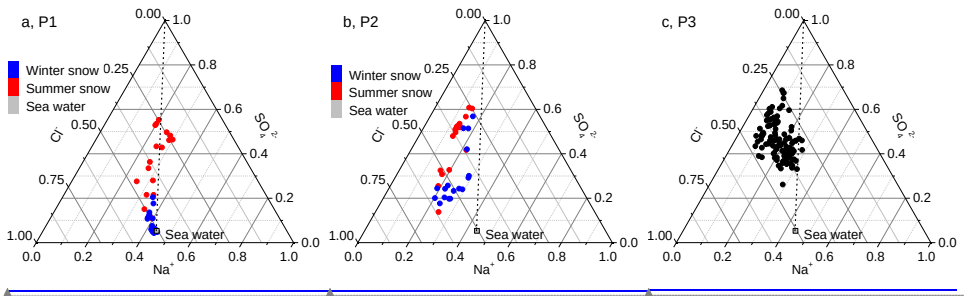

Figure 12. The same as Fig. 7, with blue and red dots in panels (a) and (b) representing winter and summer snow, respectively.

带格式的：字体：小五

带格式的：字体：小五

带格式的：字体：10 磅

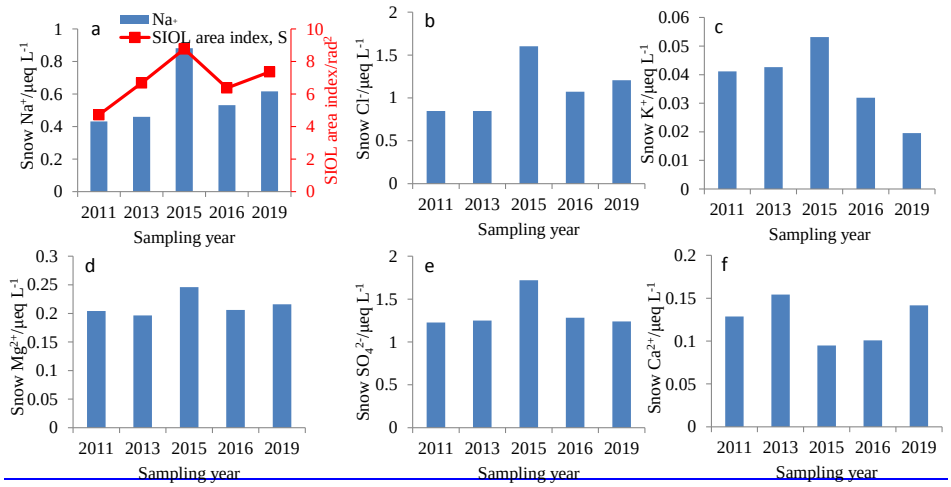

~~Figure 13.~~ ~~Averaged ion concentrations in surface snow collected on the traverse in different years. The area index of the Southern Indian Ocean low (SIOL), S, is shown in panel (a), calculated following~~ **~~错误!超链接引用无效。~~** ~~. The mean sea level pressure from ERA-interim reanalysis during the austral summers in 2010/2011, 2012/2013, 2014/2015, 2015/2016, and 2018/2019 was used to calculate the values of S (Figure S3).~~